Regulatory Mechanisms in Biosystems

ISSN 2519-8521 (Print)
ISSN 2520-2588 (Online)
Regul. Mech. Biosyst.

# Specific anatomical identification of *Convallaria majalis* (Asparagaceae), a medicinal plant with a sciophytic character

A. Sardarova

*Azerbaijan State Agricultural University, Ganja, Azerbaijan*

*Article info*

*Received 02.06.2025*
*Received in revised form 22.06.2025*
*Accepted 16.07.2025*

*Azerbaijan State Agricultural University, Ozan st., Ganja, AZ2007, Azerbaijan. Tel.: +994-506-044-442. E-mail: aygun.sardarova4442@gmail.com*

***Sardarova, A. (2025). Specific anatomical identification of Convallaria majalis (Asparagaceae), a medicinal plant with a sciophytic character. Regulatory Mechanisms in Biosystems, 16(3), e25140. doi:10.15421/0225140***

The aim of this study is to identify the specific anatomical diagnostic features and structural adaptations of *Convallaria majalis* in accordance with its ecological group, based on anatomical investigations of its vegetative organs. For the first time in the flora of Azerbaijan, a comprehensive anatomical study has been conducted on *C. majalis*, providing fundamental information on its diagnostic characteristics and structural variability associated with its shade-loving (sciophytic) nature. These findings contribute significantly to the fields of biodiversity, systematics, ecology, phytogeography, and applied botany. Vegetative organs of *C. majalis* were collected and fixed for dehydration and subsequently subjected to anatomical, microscopic, histochemical, and biometric analyses. Micropreparations prepared using modern digital optical microscopes allowed tissue- and cellular-level examination, structural clarification, and acquisition of micrometric measurements. The presence of aerenchyma, a tissue associated with hypoxic regulation, was identified in the vegetative organs of *C. majalis*. As an indicator of its sciophytic character, the localization of photosynthetic compounds within the leaf mesophyll was observed. A significant scientific novelty in plant anatomy was the identification, for the first time, of a structure belonging to the "endoaerenchymal stomatal-epidermal complex" located in the pith of the stem of *C. majalis*. The theoretical and practical data obtained in this study enable the anatomical-level identification of the species by highlighting its specific features. The anatomical characteristics of *C. majalis* provide a basis for distinguishing it from closely related taxonomic groups, serving as a biomarker for the clarification of species diversity within biosystems. The identified anatomical traits reflect functional diversity within the biosystem, clearly demonstrating the role of *C. majalis* in ecosystem services. Additionally, micrographic visualizations were conducted to determine which organs show higher localization of metabolic products. These organs may be considered more effective sources of raw materials for phytotherapeutic applications in the pharmaceutical industry.

*Keywords*: unilateral endodermis thickening; polygonal xylem; lignification in phloem; idioblast; concentric type bundle; anisocytic morphological variations in mesoderm.

## Introduction

*Convallaria majalis* L., a member of the family Asparagaceae Juss., is distributed in shaded forested areas of the Republic of Azerbaijan (Qurbanov, 2024). As a newly recognized ethnobotanical resource for local communities, *C. majalis* holds promise for use in landscape design and can be introduced into shaded environments, contributing significantly to the enrichment of biodiversity. The plant's vegetative reproduction is primarily facilitated by its underground, highly branched rhizomes (Ryabchuk & Perekhodko, 2004; Kabus, 2015).

Through evolutionary processes under limited sunlight conditions, *C. majalis* has developed a small number of large leaves on its stem, optimizing light capture to enhance photosynthetic efficiency (Bessonova & Yakovleva-Nosar, 2014). The extensive and spreading rhizome system also enables the plant to store energy, thereby increasing its resilience against shade-induced stress. Anatomical traits and structural adaptations of plants are considered one of the core areas of modern botanical research, particularly for understanding their responses to ecological conditions (Saeidi Mehrvarz & Moharami, 2016; Belaeva & Butenkova, 2018; Anurag et al., 2023; Rezanejad et al., 2023). Multidisciplinary approaches that investigate plant adaptation processes at anatomical, physiological, molecular, palynological, morphological, and biotechnological levels are of particular importance for the scientific characterization of internal structures (Bulavin, 2015; Ulcay, 2022; Nyzhnyk et al., 2024; Schwartau et al., 2024).

The localization of phytochemical compounds within a plant may vary. In many species, such compounds accumulate in specific organs or tissues, often supported by specialized structures involved in synthesis and storage at the anatomical level (Popova, 2017). In this regard, *C. majalis* is noteworthy for its high accumulation of biochemical substances in all vegetative organs. Numerous studies have identified the presence of pharmacologically active compounds such as cardenolide glycosides (e.g., convallatoxin and convallatoxol), convallasaponin A, cholestane, and steroidal glycosides (Matsuo et al., 2017; Demir et al., 2022). Given that all representatives of the genus *Convallaria* possess significant medicinal value, their anatomical structure has attracted the attention of researchers from various countries (Harb et al., 2016; Boubetra et al., 2022; Sarapan et al., 2023). The rich chemical composition of *C. majalis* enhances its pharmacological significance, making it a valuable plant raw material in the treatment of cardiovascular diseases, neurocirculatory dystonia, hysteria, and mild forms of toxic goiter. It is also used in the production of choleretic and spasmolytic pharmaceutical preparations. In both classical and modern medical approaches, the plant is recognized for its cardiotonic specificity (Ibadullayeva, 2024). Due to its pharmacological potential, anatomical investigation of *C. majalis* remains highly relevant and scientifically significant. The anatomical findings from the present study align with results from previous investigations conducted by the author (Sardarova, 2024, 2025a, 2025b, 2025c; Sardarova & Ibadullayeva, 2025). Additionally, the study contributes to the broader scientific effort aimed at elucidating structural adaptations of plants under diverse environmental conditions (Bulavin, 2013; Makruf et al., 2024).

This research is of particular importance due to its application of modern, high-resolution digital microscopy to study the anatomical structure of *C. majalis*. Comparative analysis reveals that only a limited number of previous studies on this species have been conducted, and those that exist are generally dated. A review of the literature confirms that most studies to date have focused on the taxonomy of *C. majalis* and the chemical classification of its biologically active constituents, with relatively little attention given to its anatomical structure.

## Materials and methods

*Collection and laboratory processing of the material.* The plant material (Fig. 1) for this study was collected during the flowering phase from the Ganja region of the Republic of Azerbaijan. After collection, the specimens were fixed using appropriate fixation techniques as described by Huang & Yeung (2015) and Criswell et al. (2025). Following fixation, the anatomical structure of the plant was examined using modern microtechnical methods. The materials were infiltrated with paraffin (BW Blended Waxes, Inc., USA), which also served as a supporting medium during sectioning. Thin sections were then prepared using a manual microtome, and subsequent anatomical investigations were conducted. The thickness of the sections was calibrated and monitored using the micrometric adjustment screw of the modern manual microtome (Radical, RMT-5, India), allowing precise measurements in the micrometer range (Fig. 2A). Section thicknesses were consistently maintained within the range of 6–7 µm. Following sectioning, histochemical methods were applied for differential staining using specific reagents. The stains employed included safranin O, fast green, Sudan III, toluidine blue, phloroglucinol-HCl, and methylene blue (KimyaLab, Turkey). Staining was carried out in a stepwise manner using a decolorization method to ensure selective staining of tissue components. The use of sequential histological staining techniques facilitated a more precise characterization of the anatomical structural components of *C. majalis*. Safranin O, a cationic dye, selectively stained structures containing anionic compounds, particularly lignified tissues such as xylem, sclerenchyma, and sclereid fibers, rendering them red (Pradhan Mitra & Loqué, 2014). In contrast, fast green is an anionic dye that preferentially stains cellulose-rich walls of living cells, especially phloem elements (Da Silva et al., 2020; Engin et al., 2024). Sudan III, an apolar dye, was used primarily to detect lipids and other fat-containing structures (Bozdağ et al., 2016). Toluidine blue served as a test reagent for the visualization of pectin and cellulose. Phloroglucinol-HCl was employed to detect lignified tissues by staining them red. Methylene blue enhanced contrast in the sections, enabling clearer visualization of cellular structures that were otherwise difficult to distinguish. This reagent is considered essential for the detailed examination of plant tissue and cell structure. Additionally, various chemical reagents – including xylene, carboxylic acid, ethylene, formalin, and lime chloride (Mir Nauki, Russia) – were used during sample processing. These substances facilitated dehydration and further clarification of the tissue sections, contributing to the overall effectiveness of the anatomical analysis (Fig. 2B, 2C, 2D). To prepare permanent slides from the stained sections, Canada balsam (Inovating Science, USA) was used (Fig. 3B). A drop of balsam was placed on the section mounted on a glass slide, which was then covered with a cover slip. The prepared slides were placed in a special incubator with a stable temperature of 20–25 °C to ensure complete drying of the Canada balsam. Once the slides were fully cured, transverse sections of the plant were subjected to detailed microscopic analysis.


**Fig. 1.** General view of species *Convallaria majalis* and its collection site in the Ganja city area

*Microscopic analysis.* Microscopic analyses were carried out at the Department of Biology, Azerbaijan State Agricultural University, using advanced digital and versatile microscopes. Primarily, the "Carl Zeiss Axio Imager A2" microscope (ZEISS, Germany), equipped with LED illumination and specially designed objectives minimizing optical aberrations, was employed for detailed anatomical investigations (Fig. 3). This model supports multiple illumination technologies – including fluorescence, shadow, variable light, and phase contrast – allowing a wide range of contrast-enhancing techniques. The microscope's interface features automatic focusing, which combines sharp images captured at various focal depths into a fully focused composite image. The "Tile Scan" function enables high-resolution composite imaging of large sample areas. Additionally, the system automatically adjusts magnification levels, facilitating real-time measurements and integration of metric indicators into the images. Images and videos obtained during analysis were saved in various formats and could be exported to external devices via the interface. The microscope delivers high optical performance, and Zeiss AxioCam cameras are integrated into the system. Using all these versatile features, it was possible to conduct a detailed examination of structural elements, obtain micrometric measurements, carry out video documentation, and generate high-resolution microphotographs of vegetative organs from *C. majalis* specimens.

In addition, the LCD Digital Microscope NLCD-307B (Wincom Company Ltd., China) was also used for microscopic analysis (Fig. 4A, 4B). This model is equipped with a digital system and an LCD screen, allowing real-time observation of the sample directly on the display. The device supports Android-based functionality and software, enabling image and video capture. Data were stored on an SD card or transferred to a computer via USB. Software such as "MicroCapture" and "AMCap" was used for computer-based analysis. After calibration within the software, micrometric measurements were performed using precision glass micrometers. This allowed high-accuracy anatomical assessments of *C. majalis*. To achieve precise identification of the organ structures, all objective magnifications (4x, 10x, 40x, 60x, 100x) were employed during the analysis. Additionally, immersion oil (RMY, USA) was used with the 100x objective (Fig. 3A), enhancing optical resolution and contrast in microscopic images. The NLCD-307B model was primarily used during the preparation phase to assess section quality and histological staining efficiency prior to mounting the permanent slides, whereas final analyses, imaging, and metric assessments were conducted using the Carl Zeiss Axio Imager A2 microscope.

For macroscopic sample observation, stereoscopic microscopes were also employed (Fig. 4C, 4D). The Zeiss Stemi508 stereo microscope (ZEISS, Germany) features apochromatic lenses that minimize color aberration and provide distortion-free, high-clarity images. With a magnification range of approximately 6.3–50× and a stereoscopic viewing effect, this microscope enabled three-dimensional (3D) visualization of specimens. The model includes LED illumination modules from both above and below, ensuring full-field sample illumination. It is also equipped with Zeiss Axiocam digital cameras and integrates with the ZEN imaging software for image capture, brightness and contrast adjustments, manual focusing, calibration, and metric measurement. Another stereomicroscope used in the macromorphological analysis was the Stereo YK-SM067B2 model (Wincom Company Ltd., China), a binocular version with manual control. This device, with interchangeable lenses and oculars, provides a magnification range of 6.7–45×. Using the unique stereoscopic optics of these microscopes, high-resolution and detailed examination of the macroscopic structures of *C. majalis* was performed, leveraging their broad field of view and 3D visualization capabilities.

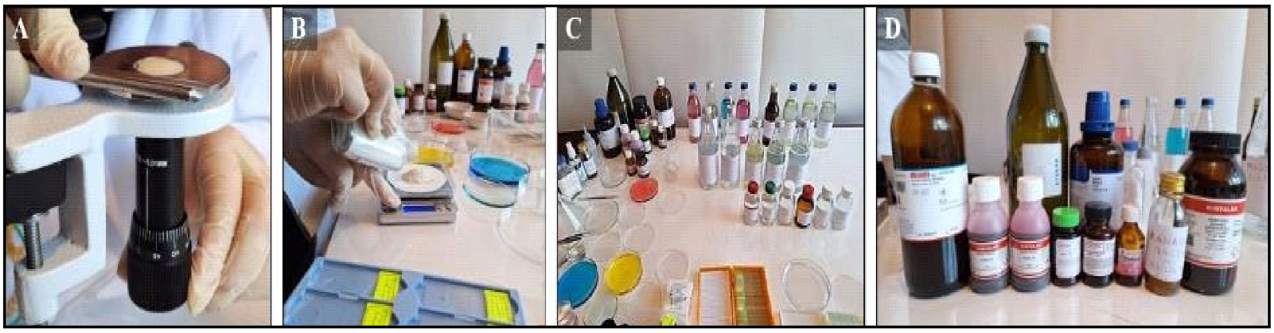

**Fig. 2.** The hand microtome (*A*) used for obtaining sections from plant samples, the process of preparing the sections (*B*, *C*), and the reagents (*D*) used


**Fig. 3.** Conducting an anatomical analysis using Axio imager A2 optical microscope model, utilizing immersion oil (*A*) in this analysis, and employing Canada balsam (*B*) in the preparation of specimens

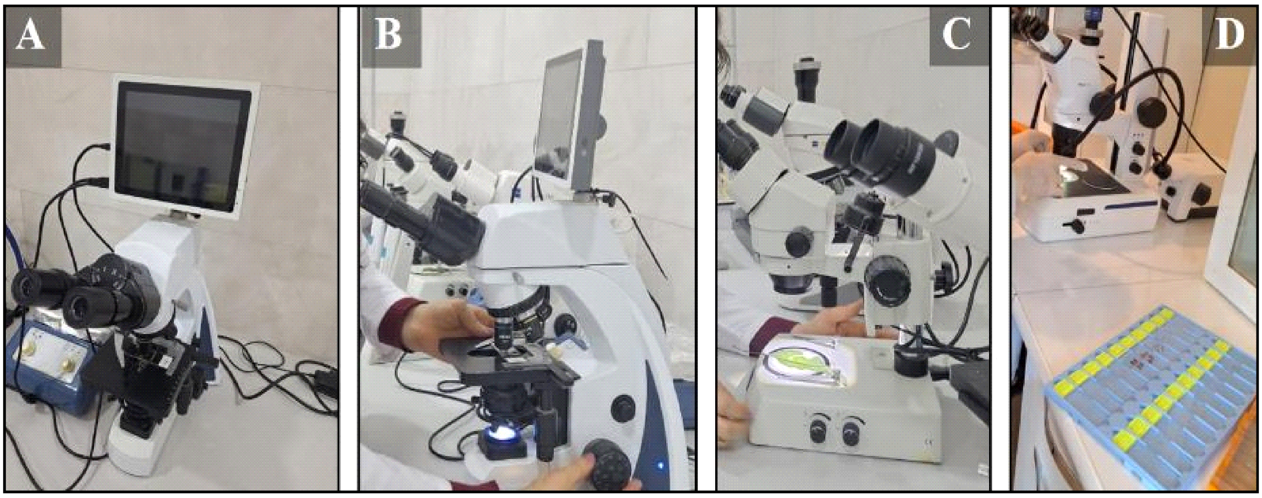

**Fig. 4.** Optical and stereoscopic microscopes used: *A*, *B* – LCD Dijital Microskop NLCD-307B; *C* – Steoroscope Zeiss Stemi508; *D* – Stereo YK-SM067B2

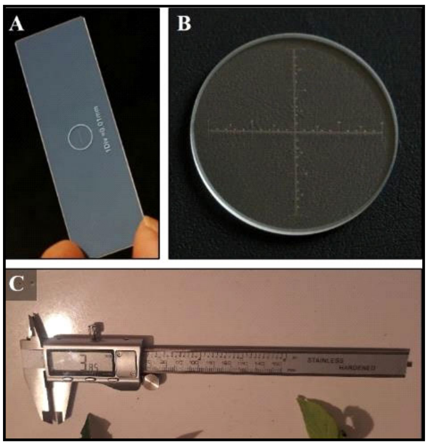

**Fig. 5.** Instruments used in the measurement process: *A* – stage micrometer; *B* – eyepiece micrometer; *C* – digital micrometer

To verify the precision of micrometric data obtained through the microscopes, both ocular and objective micrometers (Muhva, China) were used during analysis (Fig. 5A, 5B). Initially, the ocular micrometer was calibrated against the objective micrometer, after which measurements of observed structures were conducted using the calibrated scale. Additionally, a digital micrometer (Jiavarry, China) (Fig. 5C) was employed to record the macroscopic dimensions of the organs from which anatomical sections were made. The resulting measurement data were appropriately labeled on the corresponding photomicrographs (Jambor et al., 2021).

*Preparation of herbarium specimens.* The primary aim of this study is to investigate the anatomical characteristics of *C. majalis* and to identify its distinctive structural features. Documenting these anatomical traits in herbarium specimens also serves the purpose of enhancing the macroscopic identification of the species. Herbarium samples provide not only a systematic and in-depth representation of the plant's anatomy but also serve as essential reference material for evaluating the species' potential in pharmacognosy and phytotherapy.

**Fig. 6.** Preparation of herbarium

The preparation of herbarium specimens was carried out in accordance with standard scientific methodologies to ensure their systematic and long-term preservation (Uma & Düzenli, 2012). The quality of herbarium specimens is highly dependent on the stage of collection. To ensure morphological completeness, specimens were collected with all major vegetative and reproductive organs – root, stem, leaf, flower, and fruit – intact. Based on phenological stages, *C. majalis* specimens were collected during both the flowering and fruiting phases. To preserve the collected material with high quality, pressing and drying processes were carefully regulated. During pressing, plant materials were arranged between ventilated absorbent papers in special herbarium presses. As *C. majalis* contains convallatoxin, a thermolabile compound, the drying process was conducted under a controlled temperature regime (30–40 °C). Air circulation was maintained according to regulatory standards to control humidity during the drying stage. For chemical fixation of roots and rhizomes, ethanol and formalin were applied.

After the completion of these steps, the dried plant specimens were mounted on herbarium sheets, segmented as needed according to specimen size, and labeled appropriately (Fig. 6). The labeling of herbarium specimens followed the International Code of Botanical Nomenclature format. Each label included the scientific name of the species (in Latin with author citation), family and genus name (in Latin), collection location (region and coordinates), date of collection, name of collector, and herbarium code. Special attention was given to the storage conditions and preservation of the prepared herbarium materials. According to international standards, herbarium sheets were stored at a temperature of 15–20 °C and relative humidity of 40–50%. To protect against pests, fumigation was performed in accordance with international phytosanitary protocols.

The herbarium specimens prepared in the framework of this study are presented as standardized reference materials for the anatomical investigation of *C. majalis*. These specimens can serve as exemplary resources in scientific research and also act as visual teaching tools in the fields of botany, ecology, and pharmacognosy. The *C. majalis* herbarium samples have been incorporated into the herbarium collection of the Department of Biology named after Academician Valida Tutayuq at the Azerbaijan State Agricultural University. These specimens are preserved as part of a systematized botanical collection and are accessible for research, educational, and reference purposes.

*Statistical methods.* In this study, 8 to 12 individual plants were selected from *C. majalis* populations distributed in the Ganja region of the Republic of Azerbaijan. From each plant, vegetative organs were sampled for anatomical investigation. For each organ, 10 to 15 transverse sections were prepared and subjected to detailed anatomical analysis. During microscopic examination, various structural parameters were measured. All measurements were statistically analyzed using the Jamovi software (version 2.6.26, University of Sydney, Australia). Results were expressed as mean values accompanied by standard deviation (SD) to ensure the reliability and reproducibility of the data.

**Results**

*Leaf.* For the first time, our anatomical investigations revealed an atypical leaf structure in *Convallaria majalis*, characterized by a heterogeneous parenchymatous organization. The identification of a modified palisade parenchyma located in the lateral zones of the leaf—displaying an irregular dorsoventral pattern—constitutes a novel scientific finding. This irregular dorsoventral leaf anatomy features a complex tissue structure, in which laterally positioned palisade parenchyma cells coexist with centrally located isodiametric parenchyma cells, reflecting a unique evolutionary anatomical adaptation. In transverse section, the central vascular region of the leaf appears relatively angular in shape (Fig. 7A, 7B). The inner portion of this region is composed of large, isodiametric parenchyma cells. Small intercellular spaces are present where the cell walls do not adjoin. Additionally, in the expanded areas of the leaf adjacent to the central vein, some parenchyma cells undergo lysigenous degeneration, resulting in the formation of aerenchyma. However, the development of aerenchyma is less pronounced in the tissues between the vascular bundles located laterally (Fig. 7C, 7D). Within the parenchyma, a single centrally located collateral vascular bundle is directed dorsally. Anatomical observations indicate the presence of four lateral vascular bundles within the mesophyll, two of which are smaller. The isodiametric parenchyma cells extending from the central bundle toward the adaxial epidermis are notably smaller than other isodiametric cells in the region. On the ventral side, these cells undergo lignification in the subepidermal layer, forming a group of mechanical elements that provide support to the adaxial epidermis.

Due to the thinness of the mesophyll in the lateral vascular bundle regions, the ventral mechanical tissues are in direct contact with the bundles. The sclerenchymatous elements formed on the dorsal side of the vascular bundles exhibit strong sclerification and lignification, distinguishing them from other mechanical cells surrounding the xylem or the lignified cells of the subepidermal region.

In the central vein region, the circular parenchyma cells surrounding the vascular tissue are more actively involved in photosynthesis and metabolic exchange, providing a structure optimized for the storage and translocation of nutrients. A small group of sclerenchyma cells is located beneath the adaxial epidermis, while collenchyma cells are found beneath the abaxial epidermis (Fig. 7E, 7G). Compared to the lateral bundles, sclerenchyma development in the central vein region is weak, whereas the main parenchyma tissue is prominently developed. While the central vascular bundles are freely embedded within the parenchyma, the smaller lateral bundles in the narrow leaf margins are supported by mechanical cells attached to both the upper and lower epidermis. In *C. majalis*, lateral vascular bundles are surrounded by sclerenchyma tissue from both adaxial and abaxial surfaces, connecting directly to the epidermis. This anatomical configuration reflects a "sclerophilic trait" or "sclerenchymatization" process, commonly observed in plants with large foliage. It provides mechanical support for leaf elevation and increases resilience against environmental stresses.

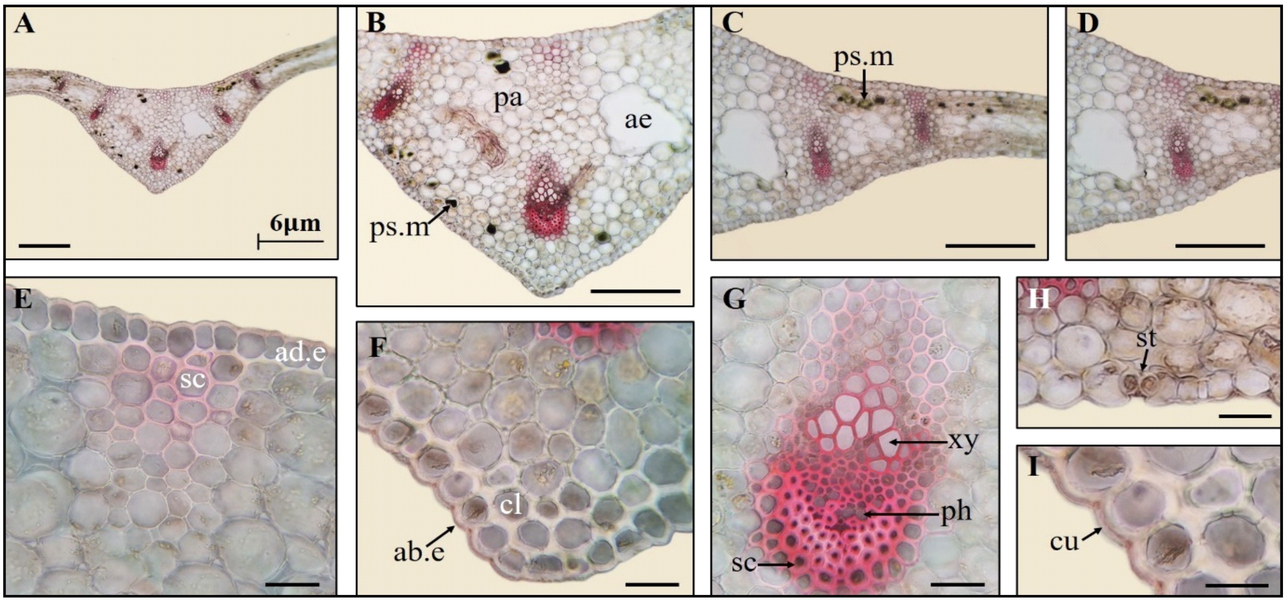


**Fig. 7.** *Convallaria majalis* (cross-section of the leaf (midrib)): *A* – general view; *B*, *C*, *D* – midrib region; *E* – sclerenchyma tissue developed in the subepidermal region of the adaxial epidermis; *F* – collenchyma tissue developed in the dorsal corner of the midrib region; *G* – collateral central bundle; *H* – stoma in the abaxial epidermis; *I* – cuticle on the abaxial epidermis; *ps.m* – photosynthetic material; *pa* – parenchyma; *ae* – aerenchyma; *sc* – sclerenchyma; *ad.e* – adaxial epidermis; *ab.e* – abaxial epidermis; *cl* – collenchyma; *xy* – xylem; *ph* – phloem; *sc* – sclerenchyma; *st* – stoma; *cu* – cuticle; scale bar: *A–D* – 500 μm; *E–H* – 50 μm; *I* – 30 μm

The surrounding circular parenchyma cells in the central vein zone facilitate water and mineral transport as well as organic substance exchange. The development of sclerenchyma in numerous lateral veins enhances the mechanical strength of the leaf, increasing resistance to hydraulic stress, moisture, and other abiotic factors (Fig. 8E). Microscopic analyses revealed that a number of phloem elements in both the central and lateral vascular systems of *C. majalis* underwent lignification, which may be interpreted as a physio-anatomical adaptation mechanism. Additionally, anatomical investigations showed that the vessel elements forming the xylem in the vascular bundles embedded within the mesophyll exhibit a distinct structural organization (Fig. 9). Microscopy revealed that in *C. majalis*, xylem vessels in the leaf and across all vegetative organs are not circular in shape but rather polygonal (e.g., quadrangular or polyangular). This structural characteristic is considered to be of ecological and physiological importance, particularly in optimizing water conduction and enhancing mechanical support.

In the peripheral regions of the mesophyll, there are horizontally aligned, 4–5 layered cells that morphologically resemble palisade parenchyma but differ in function and orientation (Fig. 8A, 8B, 8F–8H). This unusual anatomical trait in the leaf of *C. majalis* may be associated with the lack of differentiation typically observed in the isolateral leaf structure of monocotyledons. Although these cells resemble palisade parenchyma morphologically, their lateral orientation does not form a classical palisade structure. These mesophyll cells are rich in chloroplasts, indicating high photosynthetic activity. The combination of a centrally located, isodiametric parenchyma-dominated mesophyll and a palisade-like periphery forms a non-differentiated (lateral) structure, which functionally facilitates even light distribution and enhances adaptation to shaded environments. Additionally, chloroplast-rich isodiametric parenchyma cells were observed at the edge of the leaf lamina. The absence of a classical palisade arrangement and the isodiametric morphology of these cells suggest a distinct mesophyll structure in this region. Although this zone is photosynthetically active, its structural features are more similar to the central isodiametric parenchyma, morphologically differing from true palisade tissue. These findings also indicate morpho-functional zonation within the leaf mesophyll.

Despite being a monocot, *C. majalis* does not exhibit a typical isolateral leaf structure. Instead, its mesophyll displays a heteromorphological organization, with horizontally arranged palisade-like cells in the peripheral zone and centrally located isodiametric parenchyma cells surrounding the vascular bundles, extending from the adaxial to the abaxial epidermis. Due to the observed morphological and functional variation in the mesophyll, the leaf can be classified as a modified isolateral-type with a heteromorphological structure. This specialized leaf organization is likely an adaptation to mesophytic, shaded ecological conditions. *C. majalis* typically inhabits shaded and semi-shaded mesophytic ecosystems. Accordingly, the mesophyll cells are likely to accumulate photosynthetic compounds, which may represent an adaptation strategy for shade tolerance. The accumulation of green photosynthetic substances in the subepidermal layers, particularly within the main parenchyma, represents an eco-anatomical adaptation to the plant's shaded habitat (Fig. 9). The ecological conditions in which this sciophytic species develops support the formation of photosynthetically active tissues with a high chloroplast concentration. These specific anatomical features, along with the localization of metabolic products, may directly reflect the sciophytic nature of this medicinally important species. As such, these traits are considered fundamental components of *C. majalis*' bioecological strategies and contribute to its biodiversity significance. The adaxial and abaxial epidermal cells covering the leaf are relatively smaller and more compact in the central, expanded region composed of isodiametric parenchyma. Toward the peripheral regions of the mesophyll, epidermal cells become more oval and elongated along the periclinal axis. Notably, the adaxial epidermal cells in this zone appear significantly larger (Table 1). The epidermis is covered by a cuticle layer, serving as a protective barrier against gas and liquid exchange.

The leaf of *C. majalis* was found to be amphistomatic, with stomata present on both the adaxial and abaxial surfaces of the epidermis. Microscopic analysis revealed that the stomata are of the anomocytic type, characterized by the absence of distinct subsidiary cells surrounding the guard cells (Fig. 7H, 7I, 9I). However, the cells neighboring the stomata, although not structurally differentiated as true subsidiary cells, were observed to be significantly larger than the surrounding epidermal cells. The guard cells were positioned in depressions between these larger epidermal cells, partially sunken into their surface. In the lower corners of the central expanded region of the leaf lamina, a small amount of collenchyma tissue consisting of one or two layers of cells was observed in the subepidermal layer. However, collenchyma tissue was absent in the lateral extremities of the leaf. At these terminal regions, the adaxial and abaxial epidermal layers were found to converge and connect through 5–7 tightly packed epidermal cells whose inner walls were in direct contact with each other.

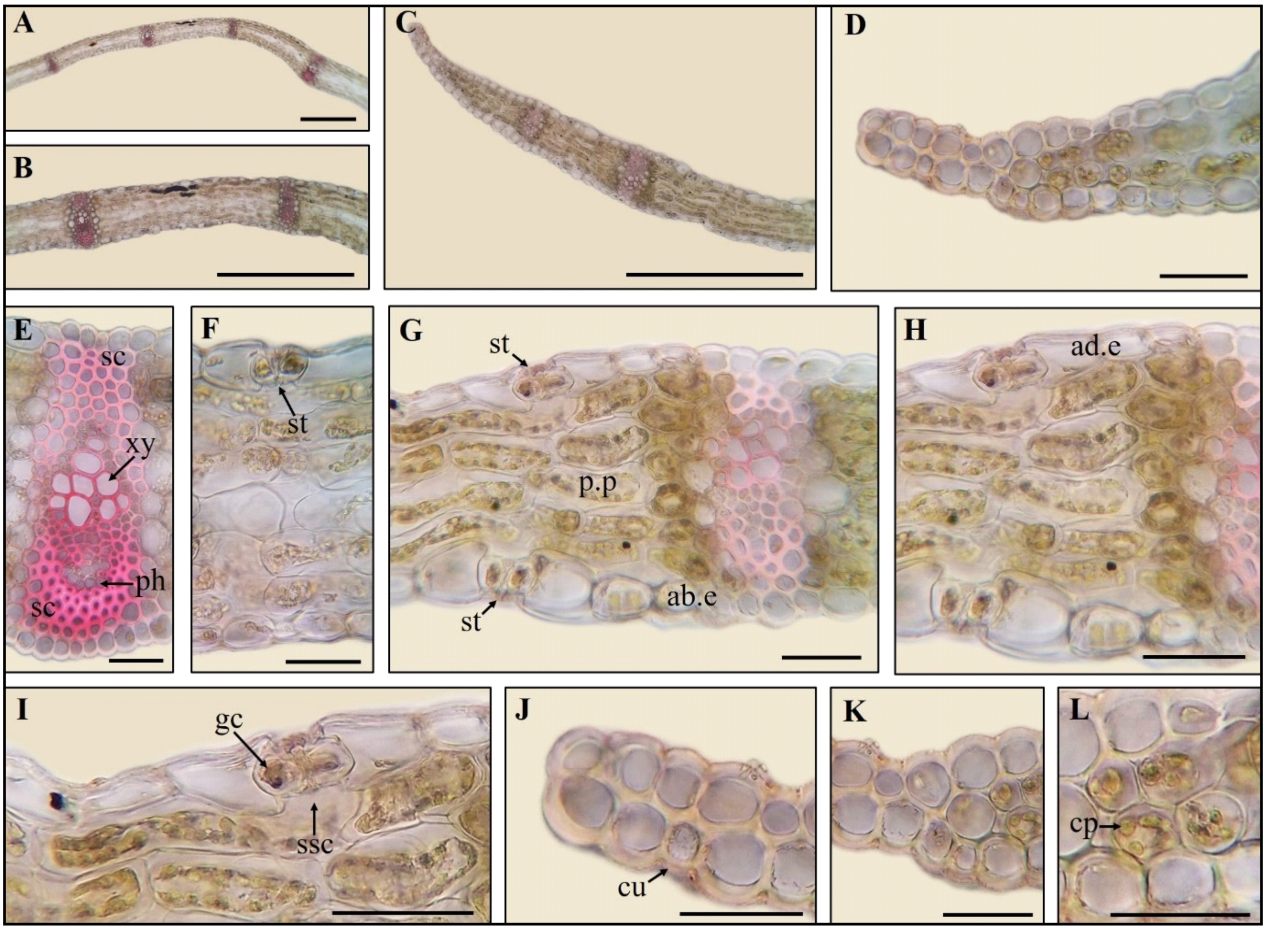


**Fig. 8.** *Convallaria majalis* (cross-section of the leaf (lateral bundles)): *A* – lateral bundles in the mesophyll; *B*, *C* – parts of mesophyll; *D* – margin region; *E* – lateral vascular bundle; *F*, *G* – structure of the mesophyll; *H* – horizontally oriented palisade cells, which are delimited by isodiametric cells near the lateral bundle, *I* – adaxial stoma; *J*, *K* – margin region; *L* – chloroplast-containing parenchyma; *xy* – xylem; *ph* – phloem; *sc* – sclerenchyma; *cu* – cuticle; *ad.e* – adaxial epidermis; *ab.e* – abaxial epidermis; *p.p* – palisade parenchyma; *st* – stomata; *gc* – guard cells; *ssc* – sub-stomatal cavity; *cp* – chloroplast; scale bar: *A–C* – 500 µm; *D–I* – 50 µm; *J–L* – 30 µm

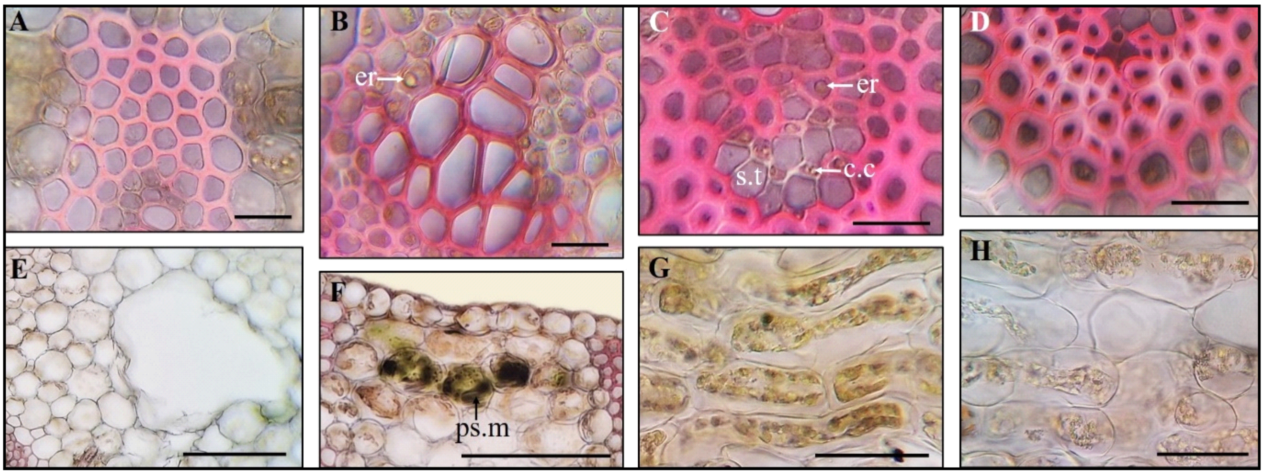


**Fig. 9.** *Convallaria majalis* (cross-section of the leaf): *A* – sclerenchyma tissue surrounding the xylem; *B* – polygonal xylem vessels; *C* – lignification in phloem; *D* – sclerenchyma tissue surrounding the phloem; *E* – aerenchyma in the midrib region; *F* – intracellular metabolites appearing green; *G*, *H* – partially differentiated cells in the mesophyll; *er* – ergastic substances; *s.t* – sieve tube; *c.c* – companion cell; *ps.m* – photosynthetic material; scale bar: *A–D* – 30 µm; *E–H* – 200 µm

Microscopic sections of the marginal region of the leaf lamina (Fig. 8C, 8D, 8J–8L) revealed that the epidermal cells in this area are oval-shaped, have thick cell walls, and are densely arranged. These cells are covered by a prominent and well-developed cuticle layer, which serves as a critical morpho-functional adaptation for reducing water loss, especially in humid environments that may experience transient periods of high evaporation. The pronounced thickness of the cuticle and the compact nature of the thick-walled epidermal cells suggest that *C. majalis* possesses effective water retention mechanisms, even under shaded conditions where temporary water deficit may occur. Furthermore, this epidermal structure contributes to the mechanical protection of the leaf surface, enhancing its resistance to abiotic stress factors. The thick cuticle acts not only as a physical barrier to desiccation but also as a protective layer against environmental fluctuations, reinforcing the ecological adaptability of the species in mesophytic, shaded habitats.

**Table 1**
Quantitative characteristic of the leaf of *Convallaria majalis* (µm)

| Indicators | | Mean ± SD |
|---|---|---|
| The height of the epidermis cells | abaxial epidermis | 30.26 ± 2.97 |
| | adaxial epidermis | 35.64 ± 3.43 |
| The thickness of the cell outher walls | abaxial epidermis | 3.18 ± 0.16 |
| Palisad parenchyma cells | height | 36.53 ± 3.64 |
| | width | 56.87 ± 4.83 |
| İsolateral parenchyma cells | | 97.56 ± 6.15 |
| Aerenchyma | | 253.63 ± 20.21 |
| Central bundle | | 245.07 ± 8.57 |
| Lateral bundle | | 127.64 ± 7.29 |
| Xylem vessel wall thickness | | 1.12 ± 0.08 |

*Petiole.* A number of distinct structural features have been identified in the petiole of *C. majalis*. In the central part of the petiole, a thickening is observed, forming a conical protrusion that extends downward. Microscopic observations indicate that, in addition to large-sized vascular bundles, relatively smaller bundles are also present within the petiole (Fig. 10A–10F). A characteristic anatomical feature of the *C. majalis* petiole is the well-developed structure of the vascular bundles located at the terminal parts of its wings, as revealed by detailed microscopic analysis (Fig. 10G–10J).

Microscopic analyses revealed the accumulation of fine ergastic and constitutive substances in the parenchyma of the petiole, as well as in the cells of both the lower and upper epidermis. Thickening of the inner and outer periclinal walls, and to a lesser extent, the anticlinal walls of the lower epidermal cells, was recorded. These cells appeared somewhat columnar in shape. In contrast, the smaller, isodiametric upper epidermal cells exhibited only slight wall thickening (Table 2). Notably, at the terminal portions of the petiole wings, the cells of the upper epidermis resembled those of the lower epidermis and showed evidence of wall thickening. A well-developed cuticular layer was observed over both epidermal layers in these regions of the petiole. Furthermore, collenchyma tissue developed in the subepidermal zone where the upper and lower epidermal layers converge. This mechanical tissue, characterized by uniformly thickened cell walls, was also present in the central region of the petiole, particularly in the subepidermal zone of the lower corners (Fig. 10K–10O).

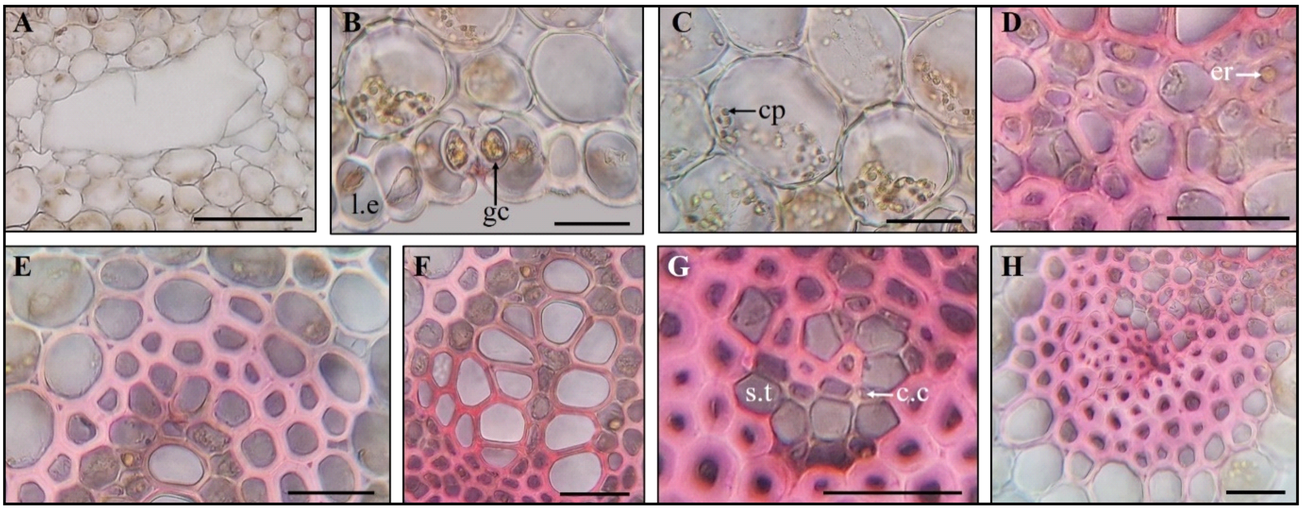


**Fig. 10.** *Convallaria majalis* (cross-section of the petiole): *A* – aerenchyma between the vascular bundles; *B* – stomata located in the lower epidermis; *C* – chloroplast-containing cells in the lower subepidermal region; *D* – ergastic substrances in the lignified phloem; *E* – sclerenchyma tissue surrounding the xylem; *F* – polygonal xylem vessels; *G* – phloem elements; *H* – sclerenchyma tissue surrounding the phloem; *er* – ergastic substances; *s.t* – sieve tube; *c.c* – companion cell; *gc* – guard cells; *cp* – chloroplast; scale bar: 30 µm

In the parenchyma tissue located between the vascular bundles, aerenchyma was formed. Plastids were accumulated in the parenchyma cells adjacent to the lower subepidermal region. These organelles are known to play a significant role in regulating metabolic processes in plants. Consequently, the intercellular spaces near metabolically active cells were enlarged. Additionally, the presence of stomata in the epidermal layer, which enhance the efficiency of aeration, was detected during analysis. Microscopic observation of the stomatal apparatus showed that the subsidiary cells were relatively larger in size (Fig. 11A–11C).

**Table 2**
Quantitative characteristic of the petiole of *Convallaria majalis* (µm)

| Indicators | | Mean ± SD |
|---|---|---|
| Upper epidermis cells | height | 33.25 ± 4.32 |
| | width | 33.87 ± 6.77 |
| Lower epidermis cells | height | 37.63 ± 8.34 |
| | width | 21.50 ± 5.80 |
| Parenchyma cells | | 78.65 ± 2.91 |
| Aerenchyma | | 262.73 ± 23.57 |
| Large bundle | | 278.93 ± 25.86 |
| Small bundle | | 106.29 ± 28.72 |

Below the fibrous-vessel vascular bundles in the petiole, groups of sclerenchymatous elements surrounding the phloem tissue were identified. These mechanical fibers exhibited significant thickening and lignification of the cell walls. The mechanical elements were also observed in three to four layers around the xylem vessels within the vascular bundle. The lignified cells around the xylem were larger than those around the phloem, although their secondary wall thickening was less pronounced. The entire vascular system of the petiole was composed of tightly arranged, polygonal xylem vessels, which may be associated with structural adaptations contributing to its functional efficiency. In *C. majalis*, the phloem tissue contained thick-walled, lignified, and sclerified cells – features that may be attributed both to adaptation to shaded environments and to genetic characteristics. These features reflect the phloem's adaptation to mechanical stress and ecological stress factors in low-light conditions. The partial lignification of certain phloem elements, as a differentiated structural feature, is believed to facilitate the more regulated transport of substances. Moreover, the presence of granulated substances in the lignified phloem elements and in small parenchymal cells within the vascular bundles was observed, likely representing an adaptive trait to shaded environments (Fig. 11D–11H).

*Sheath.* The sheath of *C. majalis* is cylindrical in form and encircles the stem. The terminal part of the petiole merges into the sheath, and the initial development of the plant begins in this region. Therefore, the anatomical structure of the sheath resembles that of the petiole to some extent. However, in transverse section, the sheath differs by forming a continuous ring (Fig. 12A–12D). As observed in the petiole, the central vascular bundle runs along a region that expands outward from the center of the sheath. In the conical area of this expansion, a small number of collenchyma cells were observed in the subepidermal zone (Fig. 12E). Not only the walls of these collenchyma cells, but also the inner walls of adjacent epidermal cells exhibited signs of secondary thickening. Examination of the vascular bundles revealed the presence of both larger central bundles and smaller lateral bundles. These collateral bundles contain thick-walled sclerenchyma fibers near the outer surface of the sheath, grouped together. This sclerenchymatous region surrounds the phloem and merges with its lignified elements, similar to what is observed in the vascular tissues of other vegetative organs. Toward the inner surface of the sheath, polygonal xylem vessels are tightly packed together. These xylem vessels are surrounded by a small number of relatively large, thin-walled mechanical cells (Fig. 12G).

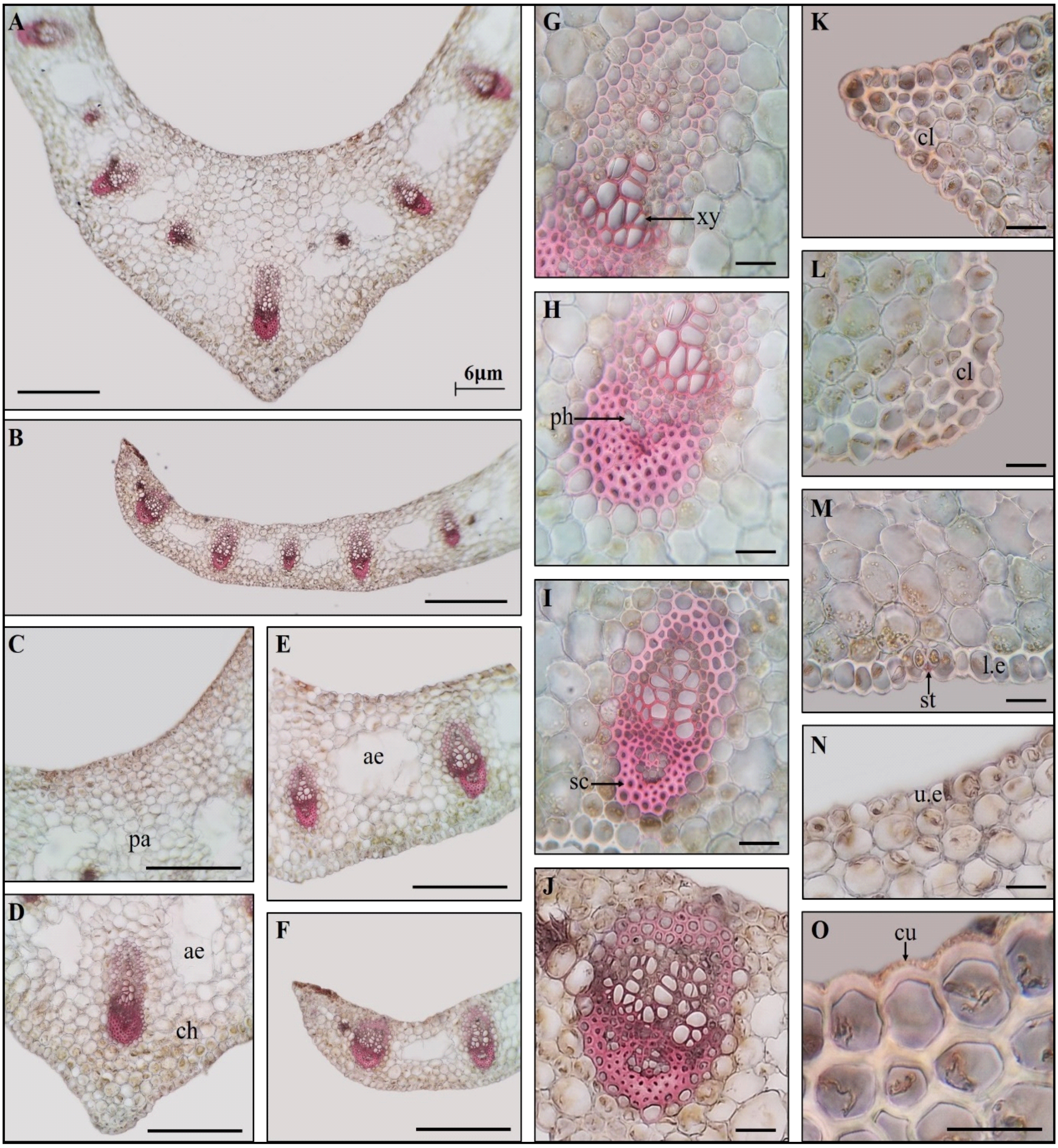


**Fig. 11.** *Convallaria majalis* (cross-section of the petiole): *A* – general view; *B* – petiole wing; *C–F* – parts of the petiole; *G*, *H* – central bundle; *I*, *J* – lateral bundles; *K*, *L* – regions where collenchyma develops; *M* – lower peripheral part; *N* – upper peripheral part; *O* – thickening of the cell walls in the epidermis; *pa* – parenchyma; *ch* – chloroplast-containing parenchyma; *ae* – aerenchyma; *xy* – xylem; *ph* – phloem; *sc* – sclerenchyma; *cl* – collenchyma; *st* – stomata; *l.e* – lower epidermis; *u.e* – upper epidermis; *cu* – cuticle; scale bar: *A–F* – 500 µm; *G–N* – 50 µm; *O* – 30 µm

The outer surface of the sheath is covered by epidermal cells that are somewhat elongated anticlinally and arranged compactly in a columnar fashion. In addition, smaller and narrower cells are also present among these epidermal cells. Beneath this outer epidermis, the subepidermal zone is composed of parenchyma cells containing chloroplasts. Accumulation of ergastic and constitutive substances was also observed both in the parenchyma tissue and in the outer epidermal cells. Similar to the petiole, thickening of the periclinal cell walls and comparatively weaker thickening in the anticlinal walls was detected in the outer epidermis under microscopic analysis. Stomata were present in the outer epidermis; their subsidiary cells were larger than the surrounding epidermal cells, enclosing the guard cells. Each guard cell was somewhat sunken toward the interior of its associated subsidiary cell and is rich in chloroplasts. Anatomical analysis revealed that air chambers were formed beneath these stomata (Fig. 12H, 12I).

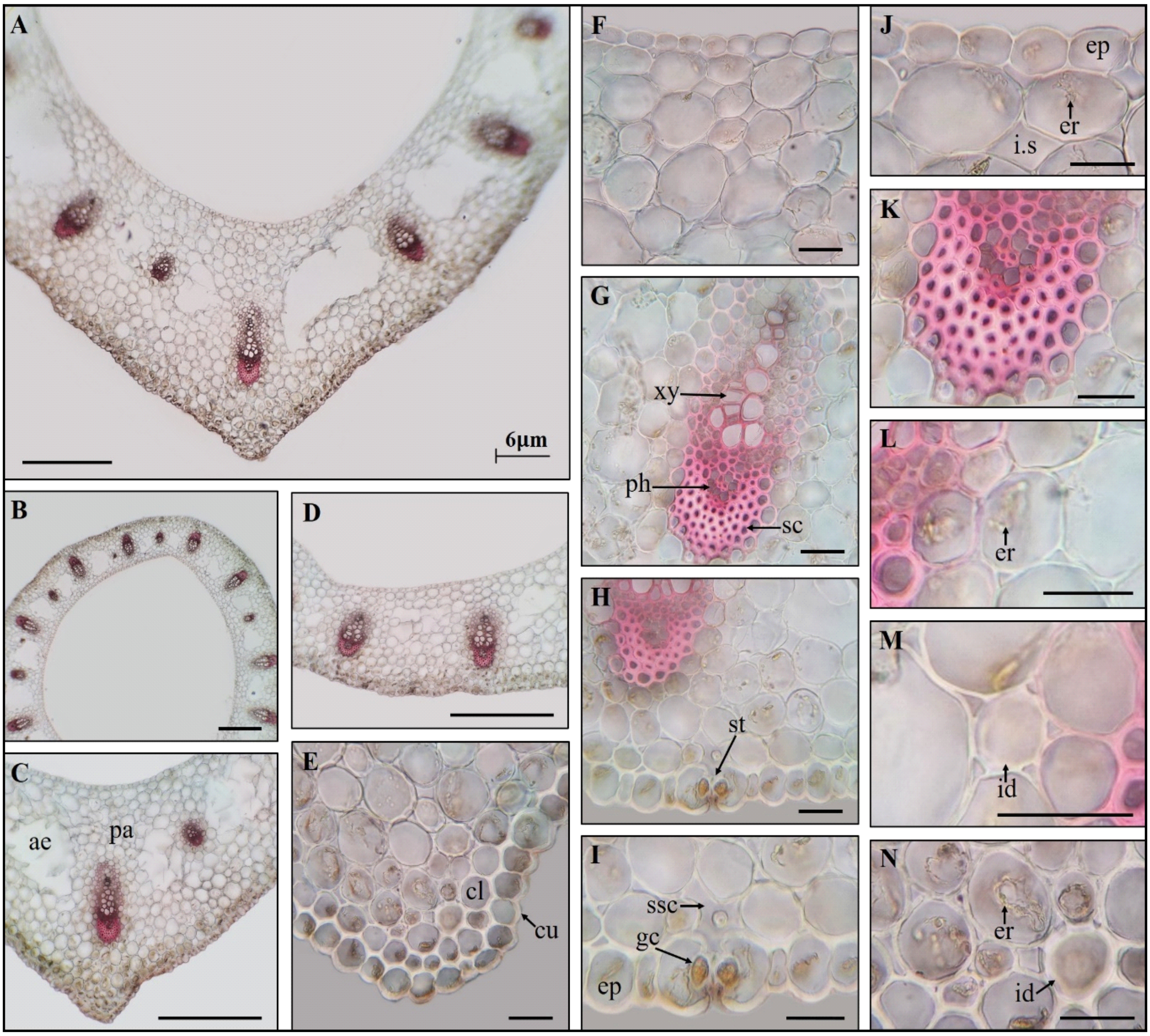


**Fig. 12.** *Convallaria majalis* (cross-section of the sheath surrounding the stem in the adult phase): *A*, *B* – general view of the cylindrical sheath; *C*, *D* – centrally located bundle region expanded towards the outside; *E* – lateral bundles region; *F* – inner side covered with thin-walled epidermal cells; *G* – collateral vascular bundle; *H* – outer side covered with epidermal cells having thickened walls; *I* – stoma; *J* – ergastic substances in the epidermal cells located on the inner side and in the parenchyma cells of the subepiderma region; *K* – sclerenchyma tissue surrounding the phloem; *L* – ergastic substances in the parenchyma cells at the boundary with sclerenchyma; *M* – idioblast-type parenchymatous secretory cell at the boundary with sclerenchyma; *N* – ergastic substances in the parenchyma cells at the boundary with collenchyma; *ae* – aerenchyma; *pa* – parenchyma; *cl* – collenchyma; *cu* – cuticle; *xy* – xylem; *ph* – phloem; *sc* – sclerenchyma; *st* – stomata; *ep* – epidermis; *ssc* – sub-stomatal cavity; *gc* – guard cells; *er* – ergastic substances; *i.s* – intercellular space; *id* – idiolast; scale bar: *A–D* – 500 µm; *E–H* – 50 µm; *I–N* – 30 µm

In the sheath of *C. majalis*, the inner epidermis exhibits distinct cellular characteristics. The cells here are smaller and tend to be elongated or oval in shape in the periclinal direction, rather than anticlinal, unlike those in the outer epidermis (Table 3). These inner epidermal cells are mostly uniform in size and shape, with no apparent wall thickening, and contain relatively fewer ergastic and constitutive substances. A small number of ergastic substances were also observed in the parenchyma cells located in the subepidermal region of the inner epidermis and near the vascular bundles (Fig. 12F, 12J–12L). The thin-walled parenchyma cells are large and isodiametric in shape. Microscopic observations showed the presence of numerous intercellular spaces among these cells. Furthermore, separation of these cells in the areas between vascular bundles led to the formation of aerenchyma tissue characterized by large air cavities.

Microscopic observations revealed the formation of idioblastic structures among the parenchyma cells located adjacent to the collenchyma tissue and in contact with the sclerenchyma of the vascular bundles in the sheath region (Fig. 12M, 12N). In the microscopic images, the presence of large, thin-walled cells containing a clear, whitish liquid in their central region was noted in the sheath of *C. majalis*. These cells are most likely idioblasts that store a specific type of liquid substance.

**Table 3**
Quantitative characteristic of the sheath surrounding the stem in the adult phase of *Convallaria majalis* (µm)

| Indicators | | Mean ± SD |
|---|---|---|
| Upper epidermis cells | height | 24.91 ± 3.86 |
| | width | 33.64 ± 4.58 |
| Lower epidermis cells | height | 45.34 ± 4.19 |
| | width | 33.55 ± 5.70 |
| The thickness of the epidermis cell outer walls | upper epidermis | 1.79 ± 0.21 |
| | lower epidermis | 4.15 ± 0.72 |
| Parenchyma cells | | 81.48 ± 9.92 |
| Aerenchyma | | 453.47 ± 36.87 |
| Large bundle | | 242.32 ± 28.96 |

*Stem.* Transverse sections of the investigated stem of *C. majalis* reveal a smooth surface and a circular outline. The main body of the stem is composed predominantly of parenchyma cells with isodiametric morphology (Fig. 13A). The vascular bundles, which constitute the conducting tissue, are located close to the epidermis. In regions near the vascular bundles, where the parenchyma consists of relatively larger cells, aerenchyma formation is evident (Fig. 13B; Table 4). In addition to the intervascular aerenchyma, a slit-shaped air cavity is also present in the central part of the stem. Unlike the intervascular aerenchyma, this central cavity is internally lined by epidermal-like cells. Around this cavity, the parenchyma cells appear to be more regularly arranged and exhibit smaller dimensions (Fig. 13C–13E). The presence of aerenchyma in the stem of *C. majalis* likely plays a key role in regulating gas exchange within the plant tissues.

The stem is externally covered by an epidermal layer composed of densely arranged, somewhat columnar cells. Microscopic analysis indicates pronounced thickening of both the inner and outer periclinal walls of these cells, which is interpreted as a structural adaptation developed by the plant in response to environmental conditions (Fig. 13F, 13G). The epidermal cells surrounding the central aerenchyma cavity are smaller, rounder, and possess thin walls. Stomatal structures were detected in both epidermal layers during microscopic examinations (Fig. 13N, 13O). The vascular bundles of the stem are of the bicollateral type and are surrounded by several layers of small, lignified cells with thickened walls. In the peripheral region of each bundle, sclerenchymatous fibers were observed enveloping the phloem. These fibers are distinguished by strong secondary wall thickening and lignification, setting them apart from other mechanical elements around the bundle. Additionally, the phloem tissue adjacent to the sclerenchyma exhibited partial lignification. As in other vegetative organs, the xylem elements within the vascular system of the stem display an angular structural configuration (Fig. 13H).

**Table 4**
Quantitative characteristic of the stem of *Convallaria majalis* (µm)

| Indicators | Mean ± SD |
|---|---|
| The height of the outer epidermis cells | 39.26 ± 6.35 |
| The thickness of the outer epidermis cells outer walls | 5.79 ± 0.41 |
| The height of the inner epidermis cells | 18.50 ± 3.75 |
| The thickness of the inner epidermis cells outer walls | 1.95 ± 0.36 |
| Cortex parenchyma cells | 54.23 ± 13.59 |
| Pith parenchyma cells | 51.78 ± 12.05 |
| Aerenchyma | 112.89 ± 27.15 |
| İntercellular space | 13.64 ± 8.37 |
| Vascular bundle | 214.32 ± 20.04 |

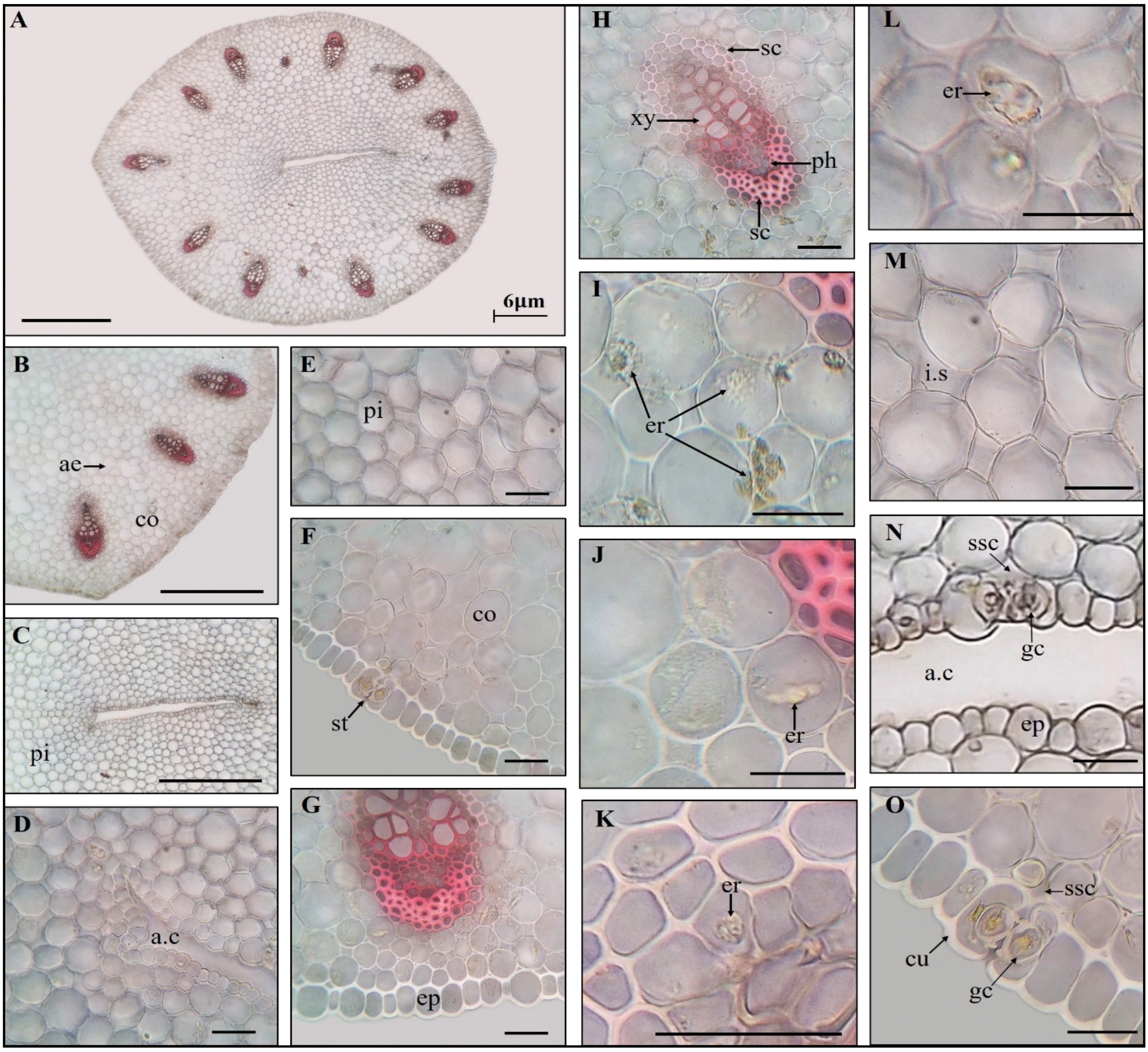


**Fig. 13.** *Convallaria majalis* (cross-section of the stem): *A* – general view; *B* – a part of the stem; *C* – pith; *D* – internal aerenchymal cavity in the pith; *E* – pith parenchyma; *F*, *G* – cortex regions; *H* – collateral vascular bundle; *I*, *J* – ergastic substances in the cortical parenchyma; *K* – ergastic substances in the xylem parenchyma; *L* – ergastic substances in the pith parenchyma; *M* – intercellular spaces in the pith parenchyma; *N* – endoaerenchymal stomatal-epidermal complex; *O* – anomocytic stomata in the epidermis covering the cortex; *ae* – aerenchyma; *co* – cortex; *pi* – pith; *a.c* – aerenchymal cavity; *st* – stomata; *ep* – epidermis; *xy* – xylem; *ph* – phloem; *sc* – sclerenchyma; *i.s* – intercellular space; *er* – ergastic substances; scale bar: *A–C* – 500 µm; *D–H* – 50 µm; *I–O* – 30 µm

Microscopic analysis of the stem of *C. majalis* revealed the accumulation of various types of ergastic and constitutive substances, as well as acicular crystals identified as raphides within the parenchyma cells. These accumulations were primarily concentrated in the cortical parenchyma cells surrounding the vascular bundles, where 3–4 distinct forms could be visually distinguished based on their morphology and size. Additionally, a limited number of medullary cells also exhibited the presence of ergastic substances (Fig. 13I–13L). In the subepidermal region of the stem, the cortical parenchyma cells are arranged more compactly beneath the outer epidermis. Toward the inner regions of the stem, these cells gradually increase in size and begin to form intercellular spaces (Fig. 13M). Together with the aerenchymatous tissue, these intercellular spaces constitute structural components that regulate the aeration processes within the internal tissues.

*Rhizome (adult phase).* The rhizome of *C. majalis* exhibits a distinct anatomical structure, which, in transverse section, is seen to be composed of a central cylinder and a cortex (Fig. 14A–14C). Microscopic analysis revealed that the outer surface of the organ is covered by an epidermis with a thick cuticle layer (Fig. 14L). Internally, beneath the epidermis, lies the cortex, within which the subepidermal cells display secondary wall thickening and differentiate into collenchyma. This thickening is particularly prominent in the region where collenchyma is in direct contact with the epidermis. In the examined rhizomes, the accumulation of small amounts of ergastic and constitutive substances was observed both in the epidermal cells and in several layers of cortical cells (Fig. 14D). The cortex is composed of medium-sized, isodiametric parenchyma cells. Numerous intercellular spaces are present between these cells, facilitating internal tissue aeration (Fig. 14J). In proximity to the central cylinder, the cortical cells abut the endodermis.

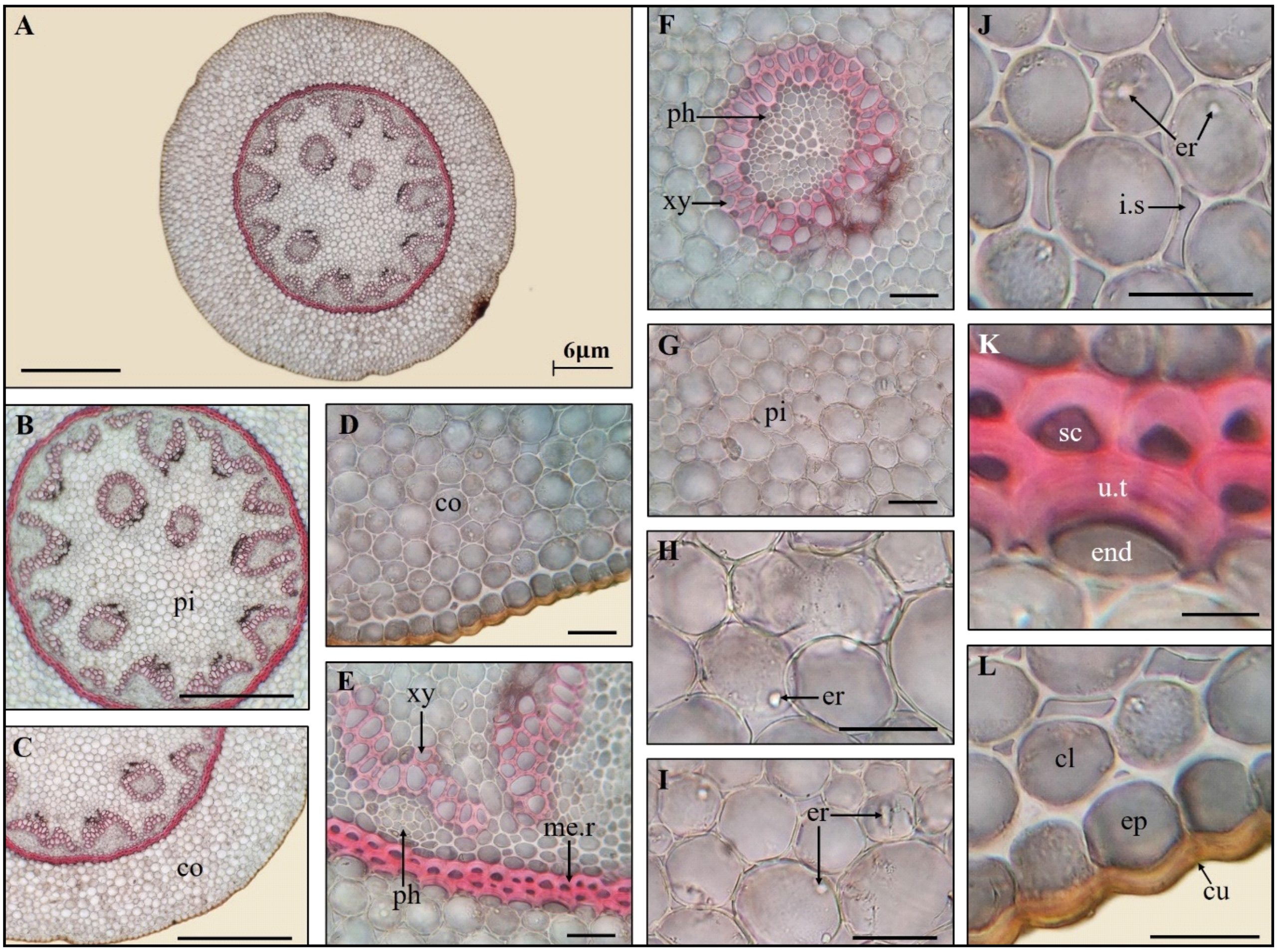


**Fig. 14.** *Convallaria majalis* (cross-section of the rhizome in the adult phase): *A* – general view; *B* – central cylinder; *C* – a part of the rhizome; *D* – cortex; *E* – semi-concentric bundles bordered by the mechanical ring; *F* – amphivasal concentric bundle in the pith; *G* – pith parenchyma; *H*, *I* – ergastic substances in the pith parenchyma; *J* – ergastic substances and intercellular spaces in the cortical parenchyma; *K* – endodermal cell with unilateral thickened wall, supported by mechanical cells from the cortex side; *L* – thick cuticle on the surface of the epidermis; *co* – cortex; *pi* – pith; *xy* – xylem; *ph* – phloem; *me.r* – mechanical ring; *i.s* – intercellular space; *er* – ergastic substances; *sc* – sclerenchyma; *end* – endodermis; *u.t* – unilateral thickened wall; *cl* – collenchyma; *ep* – epidermis; *cu* – cuticle; scale bar: *A–C* – 500 μm; *D–G* – 50 μm; *H–L* – 30 μm

In the rhizome of *C. majalis*, a high degree of sclerenchymatization was detected in the boundary zone between the endodermal layer and the adjacent sclerenchymatous ring. The cell walls affected by this process constitute approximately half of the endodermal cells (Fig. 14K). Functionally, the endodermis limits the apoplastic movement of water and dissolved substances, thereby forcing them through the cell membrane. This structural feature enables effective control of osmotic pressure and leaf transpiration. The presence of this anatomical structure in the rhizome is considered a modification of endodermal cells and holds phylogenetic significance within the field of plant anatomy. Notably, for the first time in this study, unilateral thickening of endodermal cells – interpreted as a form of synergistic interaction between the exodermis and endodermis – was observed. This species-specific feature represents a significant scientific and practical contribution to anatomical research (Table 5). Overall, the study revealed a dominance of lignification processes in various tissue groups of this species, suggesting an epigenetic regulatory strategy related to structural adaptation.

On the inner side of the mechanical tissue, the presence of a pericycle composed of one or several layers of tightly packed, small-sized cells was observed. Positioned toward the pith above the pericycle are semicentrally arranged vascular bundles, in which the xylem differentiates centripetally from the phloem groups, which vary in number. The presence of this type of vascular system in the rhizome of

*C. majalis* is characteristic of monocotyledonous plants. Microscopic observations confirm that the xylem does not form a complete ring around the phloem, although a partially concentric arrangement is visible. The xylem elements are densely packed and polygonal in shape. On the inner side of these bundles lies the pith parenchyma, within which three to four discrete vascular bundles are located. These bundles, separated from the pericycle, exhibit an amphivasal configuration, in which xylem completely surrounds the phloem (Fig. 14E, 14F). In the cells of the pith parenchyma, the accumulation of small amounts of ergastic substances, likely as a result of metabolic activity, was also observed. The parenchyma cells in this region are relatively isodiametric and exhibit small intercellular spaces between them (Fig. 14G–14I).

**Table 5**
Quantitative characteristic of the rhizome of *Convallaria majalis* in the adult phase (μm)

| Indicators | | Mean ± SD |
|---|---|---|
| Epidermis cells | height | 30.03 ± 3.98 |
| | widht | 29.87 ± 3.65 |
| The thickness of the epidermis cell outer walls | | 7.46 ± 1.02 |
| The thickness of the cuticle | | 3.63 ± 0.11 |
| Cortex parenchyma cells | | 53.13 ± 13.80 |
| Unilateral thickening of the endodermis | | 13.87 ± 1.28 |

*Pip.* In the transverse section of the pip formed on the rhizome, the internal structure reveals the presence of a juvenile-phase rhizome, an inner sheath surrounding it, and an outer sheath forming the external boundary. The juvenile-phase rhizome is distinguished from the adult-phase rhizome by its earlier developmental stage. Within the central cylinder, both semi-concentric vascular bundles located in the perimedullary region and fully developed, circular concentric bundles surrounded by pith parenchyma are observed (Fig. 15A–15D). At the boundary between the xylem of the bundles and the pith parenchyma, small cells with darkly stained, thickened walls are visible in regions directed toward the center of the cylinder. The endodermal layer surrounding the central cylinder consists of cells with slightly thickened inner walls. Immediately beneath the endodermis, one to two layers of sclerenchymatous cells form a mechanical ring, followed inwardly by the pericycle layer (Fig. 15E). Externally, the cylinder is enclosed by elements of the primary cortex. Ergastic substances were detected in both the cortical and pith parenchyma (Fig. 15F–H). The epidermal layer enclosing the cortex consists of densely packed cells with rounded or quadrangular shapes. These epidermal cells exhibit moderately thickened outer periclinal walls and are covered by a visibly distinct cuticle layer (Fig. 15I). Compared to the cuticle formed on the surface of the adult-phase rhizome, the cuticle layer here is considerably thinner. Furthermore, the thickening of the walls in the subepidermal parenchyma cells of the juvenile rhizome is less pronounced. Due to its earlier stage of development, both the unilateral thickening of the endodermis and the degree of lignification in the cells forming the sclerenchymatous ring are less advanced. Additionally, the number of semi-concentric and concentric vascular bundles within the central cylinder is lower at this stage (Table 6).

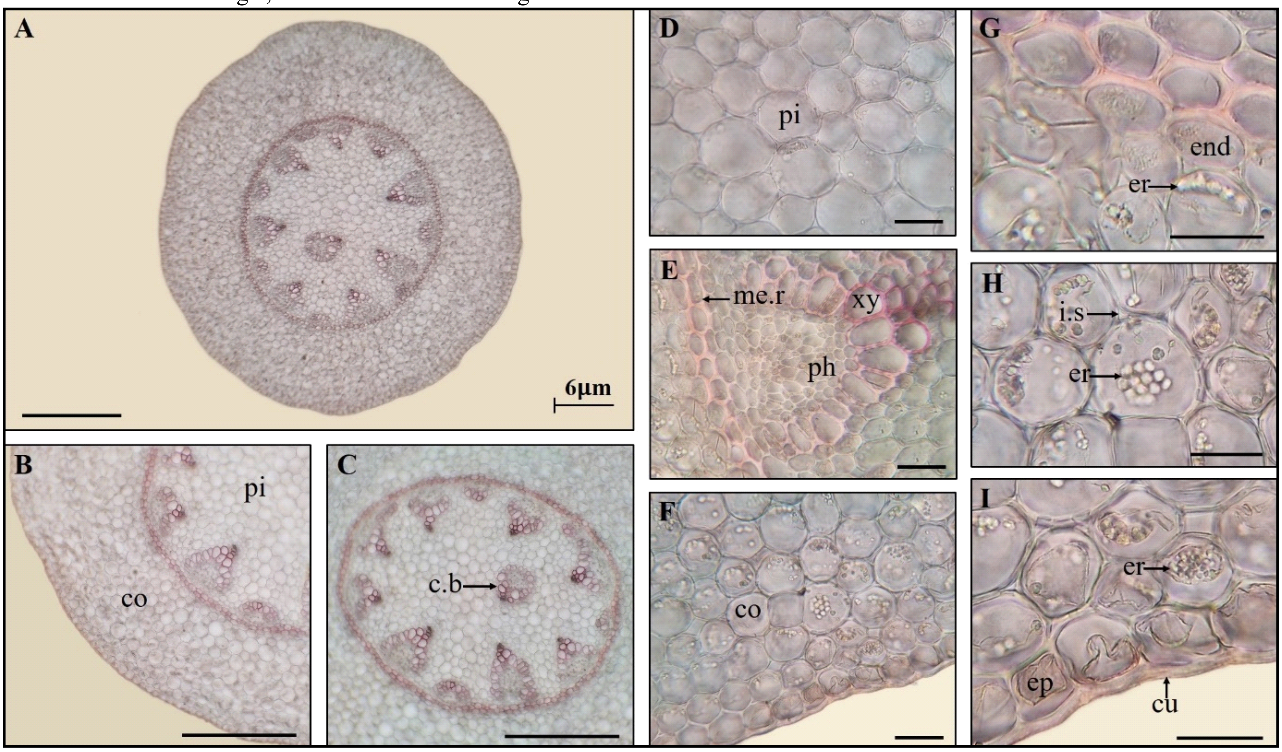


**Fig. 15.** *Convallaria majalis* (cross-section of the rhizome in the juvenile phase): *A* – general view; *B* – a part of the rhizome; *C* – central cylinder; *D* – pith; *E* – semi-concentric bundles bordered by the mechanical ring; *F* – cortex; *G* – ergastic substances in the cortical parenchyma cells near the central cylinder; *H*, *I* – ergastic substances in the cortical parenchyma and epidermis cells; *co* – cortex; *pi* – pith; *xy* – xylem; *ph* – phloem; *me.r* – mechanical ring; *er* – ergastic substances; *end* – endodermis; *i.s* – intercellular spaces; *ep* – epidermis; *cu* – cuticle; *c.b* – amphivasal concentric bundle; scale bar: *A*–*C* – 500 μm; *D*–*F* – 50 μm; *G*–*I* – 30 μm

**Table 6**
Quantitative characteristic of the rhizome of *Convallaria majalis* in the juvenile phase (μm)

| Indicators | | Mean ± SD |
|---|---|---|
| Epidermis cells | height | 33.87 ± 3.72 |
| | width | 34.14 ± 2.96 |
| The thickness of the epidermis cell outer walls | | 4.84 ± 0.52 |
| The thickness of the cuticle | | 2.18 ± 0.17 |
| Parenchyma cells | | 49.84 ± 7.15 |
| Unilateral thickening of the endodermis | | 2.87 ± 0.45 |

The juvenile-phase rhizome is surrounded by the inner sheath. Along the ring-shaped wall of this sheath, small-sized vascular bundles are located at approximately regular intervals (Fig. 16A, 16B). These bundles are arranged such that the xylem tissue is oriented toward the inner side of the sheath, while the phloem faces outward. Surrounding the vascular bundles, a small number of sclerenchyma cells with lignified walls are observed. These mechanical cells, situated around the phloem, are smaller in size and exhibit weaker secondary wall thickening compared to the sclerenchymatous cells surrounding the vascular bundles of the leaf, petiole, and stem. Aerenchyma tissue develops in the inter-bundle regions (Fig. 16E). The aerenchyma is bordered on one side by the epidermal tissue and on the other by parenchyma cells of the sheath. This epidermal layer lines the inner surface of the sheath. In cases where the aerenchyma is discontinuous, the epidermis is in direct contact with the adjacent parenchyma cells (Fig. 16C, 16D). These parenchymal cells are large and are arranged along the subepidermal zone of the outer epidermis covering the sheath. In certain regions where these cells are in contact with the inner epidermis, narrow, elongated, and angular cells are observed interspersed among them. The epidermal cells lining the inner and outer surfaces of the inner sheath differ in size and morphology. On the inner surface, the epidermal cells are narrow and elongated, with thin walls. At the points where the cells meet, their junctions appear somewhat folded in shape. A stoma is observed in this epidermal layer of the inner sheath. Its guard cells are tightly integrated with the surrounding epidermal cells. The cell walls on the adjacent sides of the guard cells are thickened (Fig. 16F). On the outer surface of the inner sheath, the epidermal cells are larger and more rounded in shape (Table 7). A cuticle layer formed on the surface of this epidermis was detected during microscopic examination. Ergastic or constitutive substances were observed accumulated in some cells of this epidermal layer. Similar deposits were also detected in parenchyma cells adjacent to the sclerenchyma surrounding the vascular bundles (Fig. 16G, 16H). In other tissues, these substances appeared only sporadically and in small amounts.

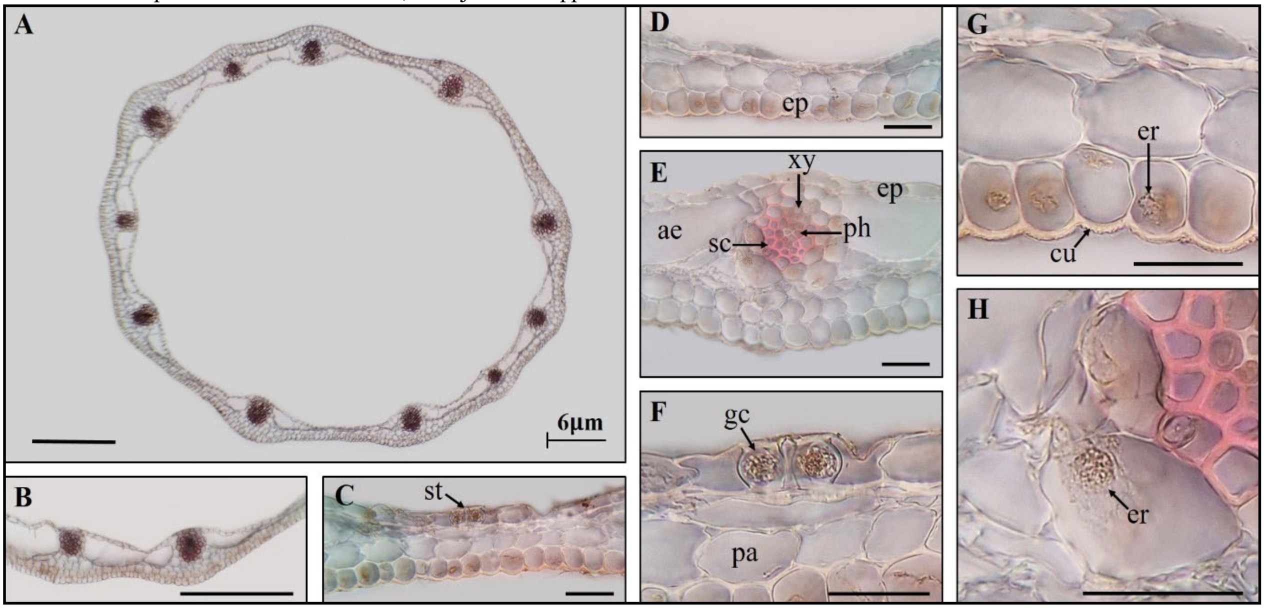


**Fig. 16.** *Convallaria majalis* (cross-section of the inner sheath surrounding the pip): *A* – general view; *B* – a part of the sheath; *C*, *D* – interbundle regions; *E* – bundle region; *F* – stoma in the epidermis lining the inner side of the sheath; *G* – accumulated substrances in the epidermis cells lining the outer side of the sheath; *H* – substances in the parenchyma cell adjacent to the vascular bundle; *st* – stoma; *xy* – xylem; *ph* – phloem; *sc* – sclerenchyma; *ae* – aerenchyma; *ep* – epidermis; *pa* – parenchyma; *gc* – guard cells; *er* – ergastic substances; *cu* – cuticle; scale bar: *A*, *B* – 500 µm; *C*–*E* – 50 µm; *F*–*H* – 30 µm

**Table 7**
Quantitative characteristic of the inner sheath surrounding the pip of *Convallaria majalis* (µm)

| Indicators | | Mean ± SD |
|---|---|---|
| Inner epidermis cells | height | 15.80 ± 2.15 |
| | width | 30.39 ± 4.07 |
| Outer epidermis cells | height | 27.96 ± 3.41 |
| | width | 20.61 ± 2.95 |
| The thickness of the epidermis cell outher walls | inner epidermis | 1.04 ± 0.19 |
| | outer epidermis | 2.25 ± 0.32 |
| Parenchyma cells | | 32.57 ± 5.23 |
| Bundle | | 114.42 ± 20.39 |

In cross-section, the anatomical structure of the outer sheath, which encloses the juvenile shoot from the outside, exhibits similar characteristics (Fig. 17A, 17B). Here, parenchymal cells are more abundant, mainly occurring in one or two layers located within the subepidermal zone of the epidermis covering the organ's outer surface, as well as surrounding the vascular bundles. In these regions, the cells of the tissue are large and polymorphic in shape. Additionally, narrow and elongated parenchymal cells are observed in areas adjacent to the inner epidermis lining the inner surface of the sheath (Fig. 17C). Microscopic analysis revealed the presence of a small amount of ergastic substances and raphide crystals in some of the large parenchymal cells (Fig. 17G). Aerenchyma tissue develops in the inter-bundle regions of the parenchyma. However, the number and size of air cavities formed within the aerenchyma are relatively lower in the outer sheath and generally appear as small-sized voids. In the structure of the vascular bundles, groups of sclerenchyma fibers encircling the phloem are observed. The phloem tissue elements are few in number and lie adjacent to the xylem, oriented toward the inner side of the sheath. The xylem tissue consists of a single row of 4–5 xylem vessels (Fig. 17D).

The epidermal cells lining the inner surface of the sheath are thin-walled, relatively narrow, and elongated in shape. Microscopic analysis revealed that in certain regions, these cells exhibit oval or somewhat rounded forms. In both the inner and outer sheaths of *C. majalis*, the epidermal cells lining the inner surfaces are tightly packed, with sinuous, interlocking contours that give the impression of being layered "on top of each other" (Fig. 17E). This interdigitated cell arrangement significantly minimizes intercellular spaces. *C. majalis* is a shade-tolerant species, typically found in low-light and humid ecosystems. Genetically adapted to develop in shaded environments, this plant requires indirect light and consistent humidity for optimal growth. The dense, undulating arrangement of epidermal cells, the relatively thin cuticle layer, and the limited number of stomata are anatomical features that reflect this ecological adaptation. The epidermal cells covering the outer surface of the sheath are relatively larger in size (Table 8). A slight thickening of their walls is observed, particularly at the boundary with the underlying parenchyma. This epidermal layer is also covered by a discernible cuticle. Stomata are present within this epidermis, but the guard cells are smaller in size compared to those found in the epidermis of the inner sheath. In addition, a small substomatal air chamber is clearly visible beneath the guard cells in this layer (Fig. 17F). In both epidermal layers of the outer sheath – and especially in the cells lining the outer surface – accumulations of ergastic and constitutive substances have been observed.

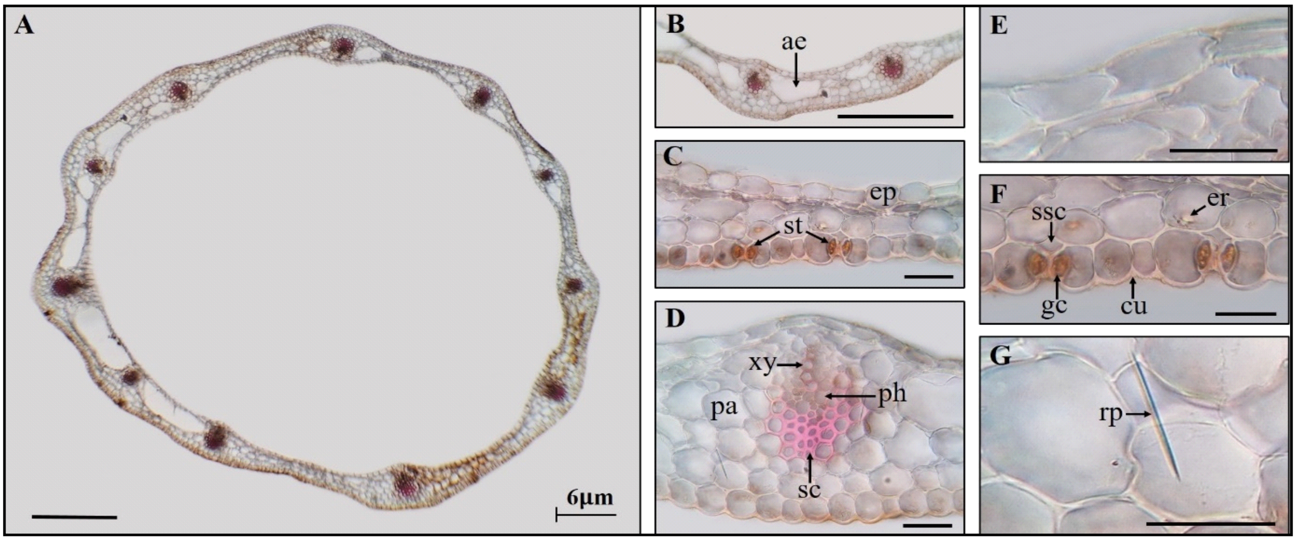


**Fig. 17.** *Convallaria majalis* (cross-section of the outer sheath surrounding the pip): *A* – general view; *B* – a part of the sheath; *C* – interbundle regions; *D* – bundle region; *E* – the epidermis lining the inner side of the sheath; *F* – stomata in the epidermis lining the outer side of the sheath; *G* – a raphide crystal in the parenchyma; *ae* – aerenchyma; *ep* – epidermis; *st* – stoma; *xy* – xylem; *ph* – phloem; *sc* – sclerenchyma; *pa* – parenchyma; *gc* – guard cells; *ssc* – sub-stomatal cavity; *er* – ergastic substances; *cu* – cuticle; *rp* – raphide crystal; scale bar: *A*, *B* – 500 µm; *C*, *D* – 50 µm; *E*–*G* – 30 µm

**Table 8**
Quantitative characteristic of the outer sheath surrounding the pip of *Convallaria majalis* (µm)

| Indicators | | Mean ± SD |
|---|---|---|
| Inner epidermis cells | height | 12.93 ± 0.89 |
| | width | 33.26 ± 1.42 |
| Outer epidermis cells | height | 32.39 ± 1.79 |
| | width | 27.71 ± 1.63 |
| The thickness of the epidermis cell outher walls | inner epidermis | 0.98 ± 0.13 |
| | outer epidermis | 2.33 ± 0.26 |
| Parenchyma cells | | 38.74 ± 2.59 |
| Bundle | | 117.98 ± 16.61 |

*Root.* In the cross-section of the root, a primary structure characterized by a polyarch radial-type central cylinder – typical for many monocotyledons – was observed (Fig. 18A). Due to the degradation of the epiblema layer in the root of the plant, the exodermis functions as a temporary protective tissue. From a theoretical standpoint, the partial disintegration of the epiblema in *C. majalis* can be attributed to its classification as a monocot species, which typically does not undergo secondary thickening and thus retains a primary root structure. However, given the perennial life cycle of the plant and its predominant propagation via rhizomes, the root structure remains in the soil for multiple growing seasons, during which its functional load may change.

Although the root retains its primary structure, age-related ontogenetic changes may lead to the degeneration of the epiblema tissue, resulting in the loss of its functional role. This process usually occurs once root elongation ceases and absorptive activity declines. In this context, although the root remains in its primary structural phase, the epiblema no longer qualifies as a "young" tissue. Functionally, the epiblema plays a role in water and mineral uptake primarily in the young root zones; however, once the root matures and transitions to functions such as anchorage or storage, the epiblema loses its functional significance. As a result, the exodermis assumes the role of a temporary protective layer (Fig. 18B, 18C). Thus, without transitioning to a true secondary structure, certain tissue layers undergo structural modifications – an occurrence particularly notable in perennial rhizomatous species, which exhibit what can be described as a “long-lived primary structure.”

Situated between the exodermis and the central cylinder is the mesodermis, which constitutes the main body of the cortex. This tissue comprises relatively large cells and is formed by polymorphic parenchyma. The outermost six to seven layers of the mesodermis are composed of large, irregularly shaped cells, while cells closer to the exodermis appear elongated, narrow, and angular in form. Directly beneath the exodermis, two to three compact layers of small, isodiametric cells are present (Fig. 18F). The mesodermis is internally delimited by the endodermis, which separates it from the central cylinder. Cells of the endodermis show slight lignification on their inner and lateral walls, particularly at points of contact with adjacent cells. This lignification, associated with the accumulation of hydrophobic lignin, allows the endodermal layer to act as a metabolic barrier, thereby restricting the movement of water and dissolved substances between the cortical parenchyma and the vascular tissues of the central cylinder. However, visual analysis revealed the presence of passage cells – endodermal cells lacking lignifications – that facilitate selective transport of substances (Fig. 18D).

Internal to the endodermis lies the pericycle, a meristematic tissue composed of a single layer of small cells. The vascular system of the root, of radial type, is located inward from the pericycle. The xylem rays include protoxylem vessels situated adjacent to the pericycle and metaxylem vessels located toward the center, embedded among mechanical tissue elements. Microscopic analyses revealed that the number of metaxylem vessels ranges between 15 and 21, while protoxylem vessels are more numerous (Table 9). The metaxylem vessels, which are several times larger than protoxylem elements, are arranged concentrically around the mechanical tissue that fills the central part of the stele. Between the xylem rays, metaphloem regions aligned with the pericycle are alternately positioned (Fig. 18E). Additionally, idioblastic cells were observed forming within the mesodermis of the root (Fig. 18G–I).

**Table 9**
Quantitative characteristic of the root of *Convallaria majalis* (µm)

| Indicators | | Mean ± SD |
|---|---|---|
| Exodermis cells | height | 48.95 ± 4.92 |
| | widht | 36.63 ± 3.88 |
| Cortex parenchyma cells | | 78.49 ± 46.77 |
| Number of metaxylem vessels | | 18 ± 3 |
| Number of protoxyloem vessels | | 49 ± 6 |

## Discussion

Anatomical, microscopic, histochemical, and statistical analyses of *C. majalis* revealed a set of specific anatomical traits reflecting its sciophytic nature. In this context, relevant international studies were also reviewed. For instance, Théroux-Rancourt et al. (2023) investigated the anatomical and physiological differences in *Vitis vinifera* leaves grown under varying light intensities.

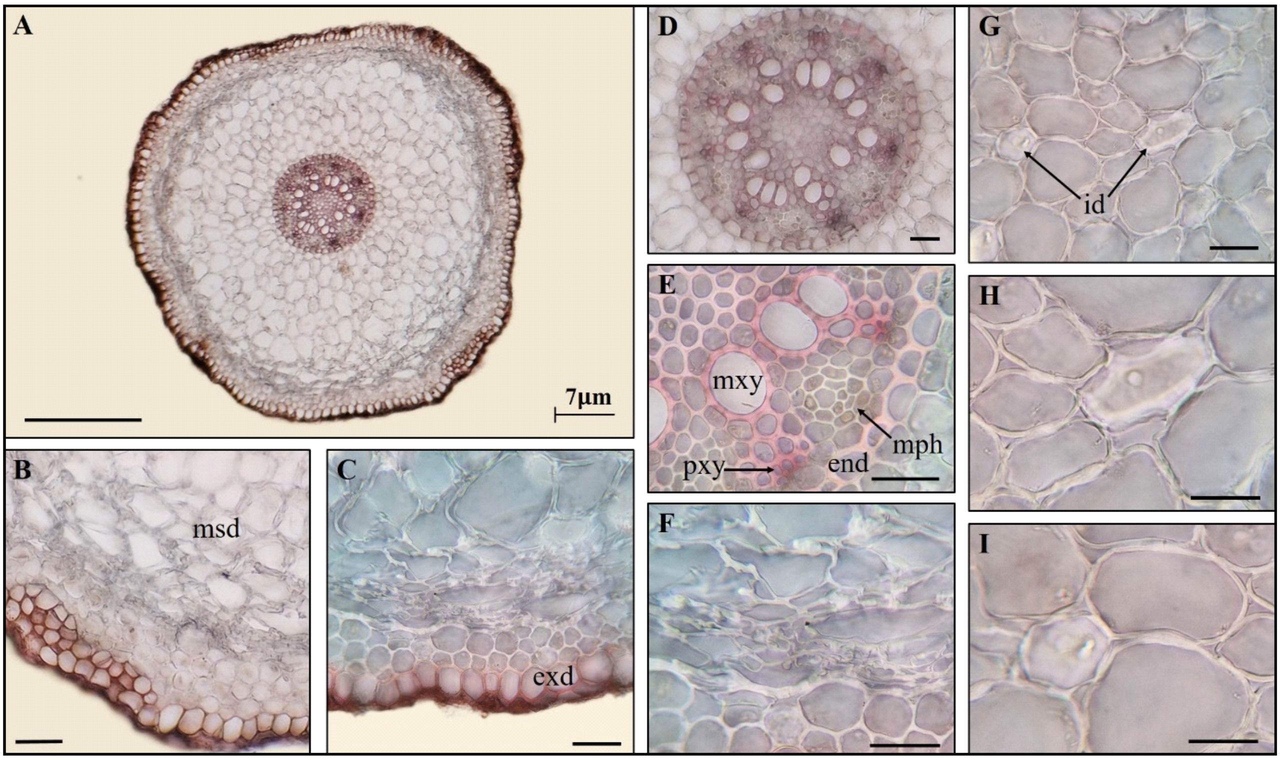


**Fig. 18.** *Convallaria majalis* (cross-section of the root): *A* – general view; *B*, *C* – parts of the cortex; *D* – central cylinder; *E* – elements of the central cylinder; *F* – anisocytic morphological variations in the mesoderm; *G* – large mesoderm cells; *H*, *I* – idioblasts in the mesoderm; *msd* – mesoderm; *exd* – exodermis; *mxy* – metaxylem; *pxy* – protoxylem; *mph* – metaphloem; *end* – endodermis; *id* – idiolast; scale bar: *A* – 500 µm; *B–D* – 50 µm; *E–I* – 30 µm

The plant material was cultivated under both shaded and full-light conditions at the BOKU UFT facilities in Austria, and the leaves were analyzed in terms of anatomical and physiological characteristics. Using micro-CT imaging, 3D structural analyses were conducted to assess leaf thickness, diffusion surface area, and other parameters. Results indicated that leaves developed under high light were thicker, had fewer stomata, and exhibited a smaller surface area of mesophyll cells. Interestingly, the number of chloroplasts within these cells was higher in plants grown under shaded conditions. Supporting these findings, our analysis of the shade-adapted species *C. majalis* confirmed the accumulation of numerous chloroplasts in both the petiole and lamina, including in isodiametric parenchymatic cells. This observation is consistent with the light-shade comparative outcomes of the foreign study.

To assess shade tolerance in *C. majalis*, a prior study by Cormack (1962) investigated morphological variability in the plant under moderate and extreme shade conditions. The author noted that under deep shade, leaves were poorly developed, smaller in size, and thinner. Anatomical analysis showed limited development of mesophyll cells, which was considered the cause of the observed morphological variation. From the perspective of ecological adaptation, these results provide a comparative basis for our anatomical findings within the flora of Azerbaijan. In our study, the lack of differentiation into a typical isolateral structure in *C. majalis* leaves – commonly seen in monocots – along with the formation of heteromorphic parenchymatic cells in the mesophyll, were interpreted as indicators of shade tolerance.

For the first time, the structural characteristics of the central vascular region and intervascular parenchyma of the *C. majalis* leaf were identified as eco-anatomical traits specific to shaded environments. These traits represent an evolutionary novelty of considerable scientific interest. The parenchyma surrounding the central vein is composed primarily of ordinary isodiametric round parenchyma cells of varying sizes (Fig. 19A), extending from both abaxial and adaxial surfaces toward the epidermis and encircling the vascular bundle. This structure supports the mechanical and physiological integrity of the vascular region. The compact and rounded morphology of the parenchyma cells is a clear morpho-functional indicator of adaptation to low-light conditions. This parenchymatic zone extends only to the area where the first lateral (bundle) vein emerges. Beyond this point, the interveinal parenchyma in the leaf blade shows a distinct morphology. Toward the leaf periphery, lateral veins are sequentially arranged, and the parenchyma between them consists of morphologically distinct cells. In these regions, 4–5 layers of elongated, columnar cells are observed. These cells are arranged horizontally, aligned parallel to one another, and resemble "collapsed" palisade layers (Fig. 19B, 19C). Thus, a classical vertical palisade differentiation is absent; however, these horizontally arranged cells contain numerous chloroplasts.

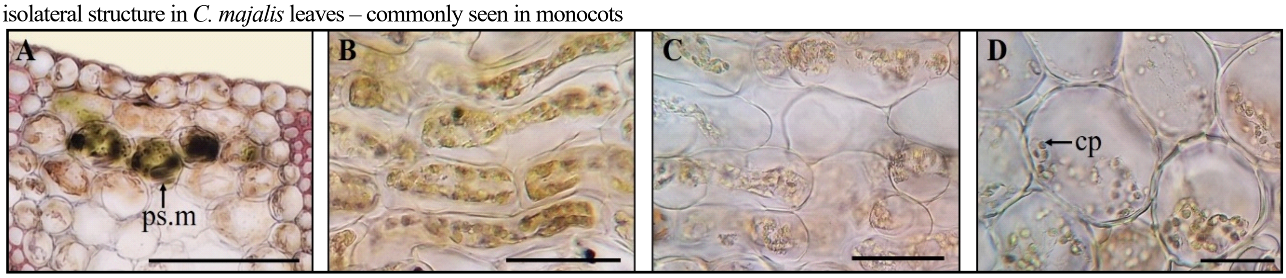


**Fig. 19.** Chloroplast-containing parenchyma tissues of *Convallaria majalis*: *A* – idioblast-type cells in the subepidermal regions of the leaf mesophyll, where photosynthetic material appears as dark green accumulations; *B*, *C* – partially differentiated chloroplast-containing parenchyma cells in the mesophyll of the leaf; *D* – chloroplast-containing cells in the lower subepidermal region of the petiole; *ps.m* – photosynthetic material, *cp* – chloroplast; scale bar: *A–C* – 200 µm; *D* – 30 µm

This unique anatomical configuration was documented in detail for the first time in our study and constitutes a novel contribution to anatomical science. The presence of such a modification in the leaf is interpreted as an adaptation to shaded environments with limited light, where maximizing the surface area of parenchymatic and photosynthetic structures is essential for regulating metabolic processes. This anatomical characteristic reflects the adaptive potential of *C. majalis* to shaded and humid ecological conditions. The specialization of parenchyma cells and morphological differentiation between tissue zones can be considered critical adaptive traits, contributing to photosynthetic efficiency, tissue elasticity, water balance regulation, and structural stability of the leaf lamina. In the mesophyll of *C. majalis* leaves, the presence of isodiametric cells from the central vein extending to the lateral vascular bundles, followed by morphologically and functionally differentiated columnar cells, clearly indicates zonal tissue organization and adaptive functional partitioning in response to shaded, humid, and mesophytic ecological conditions.

In another study conducted on this species, Kucharczyk et al. (2022) examined the anatomical effects of larval infestation by *Ctenothrips distinctus* on the leaves of *C. majalis*. Based on analyses of healthy leaves, the authors reported that the mesophyll tissue of *C. majalis* does not differentiate into distinct palisade and spongy parenchyma. In line with this observation, our findings also indicate that the mesophyll of *C. majalis* is not composed entirely of fully differentiated cells. Unlike the classical bifacial leaf type, it exhibits a weakly differentiated structure. Two major types of parenchyma cells were observed: columnar and isodiametric. The cells located beneath the adaxial and abaxial epidermis are laterally oriented, chloroplast-rich, prosenchymatous parenchyma cells. These are arranged in 4–5 layers and form a horizontally aligned, "collapsed" palisade-like structure occupying the periphery of the mesophyll. The isodiametric parenchyma cells are more prevalent around the central vascular bundle, and similar chloroplast-rich cells are found in a single layer along the lateral vascular system. Due to the absence of a spongy parenchyma layer, intercellular spaces are poorly developed. This heterogeneous and weakly differentiated mesophyll structure is a typical adaptation to shaded ecosystems. In low-light environments, maintaining a highly organized, vertically aligned palisade structure is energetically unfavorable. Instead, the broad distribution of chloroplasts among heterogeneously arranged assimilatory parenchyma cells allows the efficient capture and utilization of available light (Middleton, 2001; Dörken & Lepetit, 2018; Chen et al., 2021). This trait supports the successful growth strategy of *C. majalis* in low-light habitats. Some of the anatomical results reported by Kucharczyk et al. were also confirmed in our study. For example, the amphistomatic leaf structure and the presence of sclerenchyma tissue surrounding the vascular bundles were consistent with our findings. However, based on our microscopic observations, sclerenchymatization within the vascular bundles appeared more intense in our specimens of *C. majalis*.

The structural characteristics of sclerenchyma development along the peripheral lateral vascular system of the *C. majalis* leaf lamina were also determined. Microscopic analysis of leaves developed under shaded conditions revealed that the lateral veins are arranged in a regular and sequential manner along the periphery of the lamina. Around each vascular bundle, well-developed sclerenchymatous tissues were observed, exhibiting bifacial symmetry by extending both adaxially and abaxially into direct contact with the upper and lower epidermal layers. This vein–epidermis connection allows the vascular system to act as a mechanical support framework throughout the lamina. Strategically, such an arrangement plays a critical role in regulating tissue tension at the leaf margins and maintaining the stability of internal vascular flow. The exclusive presence of these sclerenchymatous structures in zones adjacent to the epidermis and on both sides of the vascular bundles indicates the development of a localized support system adapted to the plant's ecological conditions. This confirms that in *C. majalis*, vascular bundles within the lamina serve not only as conductive channels but also as mechanical support elements. The regular and symmetrical arrangement of these structures suggests a genetically programmed mechanism shaped by environmental adaptation.

In all vegetative organs of *C. majalis*, xylem elements exhibit trihedral, tetrahedral, pentahedral, or hexahedral forms. This is associated with their development under pressure from neighboring cells during differentiation, contributing to increased mechanical resistance (Fig. 20). Such specific features allow denser packing of xylem elements, enhancing resistance to hydrostatic pressure and optimizing hydraulic conductivity. Moreover, this structural adaptation strengthens the plant's ecological plasticity, enabling it to cope with diverse environmental stress factors and contributing to its persistence within biodiversity. The angular morphology of the xylem elements is considered a result of a specialized procambial ontogeny shaped by differential pressure from surrounding cells, marking it as an evolutionary trait in ecological anatomy. This xylem structure facilitates the acclimatization and naturalization of the shade-tolerant *C. majalis*, and plays a key role in regulating transpiration and water transport (Ružička et al., 2015; Xu et al., 2023). This unique structure holds both theoretical and practical significance for disciplines such as autoecology, plant physiology, anatomy, ecophysiology, eco-anatomy, histology, cytology, plant biotechnology, plant microbiology, and biodiversity. The formation of such species-specific features in the vascular system of *C. majalis* represents an anatomical indicator contributing to adaptive strategies, and its ecophysiological importance can be substantiated within a scientific context.

In the vegetative organs of *C. majalis*, including the leaf, petiole, stem, and sheath, partial lignification of phloem elements was observed (Fig. 21). It is well known that this species is a shade-loving plant, adapted to low-light environments. In flora representatives of the sciophyte ecological group, the development of thick-walled phloem elements tends to occur more consistently (Hardtke et al., 2008; Rajput et al., 2022). In this ecological–anatomical study, the presence of lignified phloem structures, which provide photoprotective and mechanical support functions, was identified for the first time in these vegetative organs. In low-light environments, mechanical stability and efficient water transport become more critical to maintaining assimilation and metabolic activity. Thus, the formation of lignified phloem elements under shaded conditions can be considered an adaptive response to shade tolerance. Furthermore, in a plant characterized by a stiff petiole and thick, mechanically resistant leaf blade, the development of such sclerified elements within the vascular system may also be interpreted as a genetically programmed structural adaptation (Weng et al., 2008; Voxeur et al., 2015).

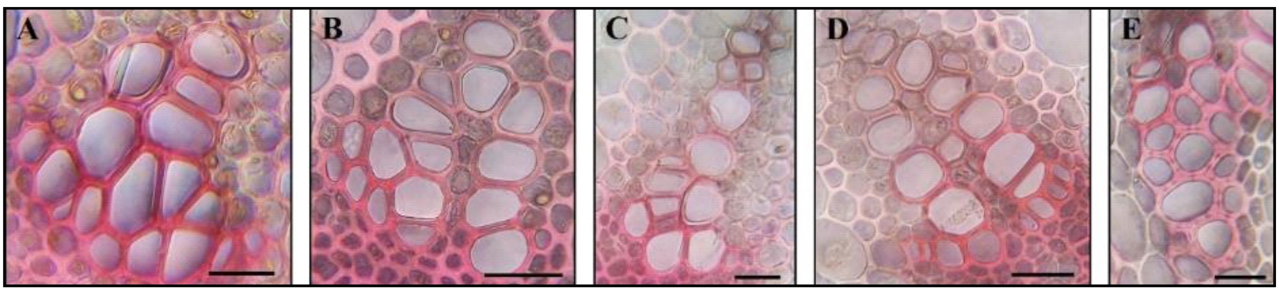


**Fig. 20.** Polygonal-structured xylem vessels of the vascular system in different organs of *Convallaria majalis*:
*A* – leaf; *B* – petiole; *C* – sheath surrounding the stem in the adult phase; *D* – stem; *E* – rhizome in the adult phase; scale bar: 30 µm

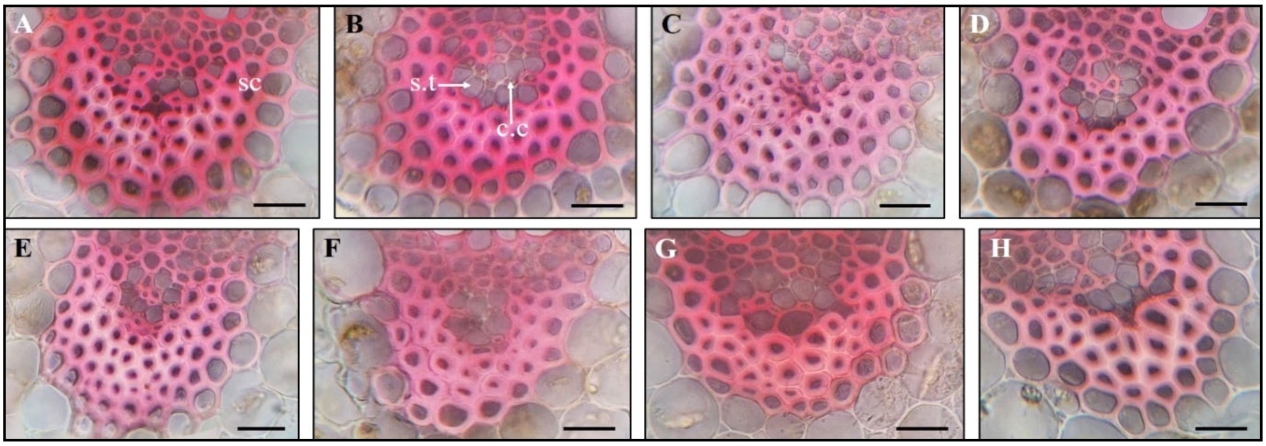


**Fig. 21.** Lignification in phloem and sclerenchyma fibres surrounding this tissue: *A*, *B* – leaf; *C*, *D* – petiole; *E*, *F* – sheath surrounding the stem in the adult phase; *G*, *H* – stem; *sc* – sclerenchyma; *s.t* – sieve tube; *c.c* – companion cell; scale bar – 30 µm

In *C. majalis*, a mesophytic species adapted to shade, the presence of aerenchymatous cavities enclosed by epidermal and stomatal structures within the pith of the stem (Fig. 22) is closely related to ecophysiological adaptation mechanisms. Considering the low light availability and continuous respiratory activity in such environments, photosynthesis is reduced while respiration persists, potentially leading to internal oxygen deficiency. The formation of aerenchymatous spaces in the pith facilitates the free movement of oxygen and carbon dioxide between cells, helping to prevent anaerobic conditions. From the standpoint of air permeability and internal ventilation, it is notable that shaded environments tend to maintain higher humidity in both soil and plant tissues. In such cases, aerenchyma and internal stomatal structures function as a ventilation system, regulating the plant's internal microclimate – a rare anatomical feature. Given the limited energy resources under low-light conditions, the formation of simplified yet functionally efficient internal air systems facilitates resource conservation. This represents an expression of structural ecophysiological adaptation. The coordination of ventilation mechanisms with the stem's pith is an evolutionary adaptation in sciophytic plants like *C. majalis*. In environments with high soil moisture and low aeration, the presence of such internal air systems facilitates gas exchange between internal and external tissues. The epidermis and stomatal apparatus act as a conduit between these internal spaces and the external environment. The discovery of an epidermal–stomatal complex within the aerenchyma constitutes a significant anatomical innovation, introduced for the first time through our research. Microscopic analysis of *C. majalis* stems revealed not only classical epidermal stomata but also uniquely isolated stomatal complexes within the internal aerenchymatous zone – an unprecedented finding in anatomical studies. The formation of internal stomata as structural and functional adaptations reflects the ecological–anatomical evolution of morpho-anatomical variation. Anatomical investigations in *C. majalis* showed that various epidermal tissues – including the adaxial and abaxial leaf epidermis, the petiole epidermis, the external and internal epidermis of the stem, the sheathing structures, and both the inner and outer sheaths enclosing the primary shoot – are all equipped with stomatal complexes. However, the morphology, density, and localization of stomata in these epidermal types vary significantly (Fig. 23).

The guard cells in the leaf epidermis are round, and their associated subsidiary cells are somewhat elongated laterally and relatively large. The cell walls of the subsidiary cells are angled and converge at the guard cells, resulting in a semi-oval shape. In the adaxial leaf epidermis, the subsidiary cells appear slightly narrower compared to those in the abaxial surface. The stomatal complexes on the petiole and the sheath surrounding the stem display a distinct morphology. In these organs, the inner and outer cell walls of epidermal cells are thickened, and the guard cells tend to assume a more oval shape. Subsidiary cells are expanded in the anticlinal direction and are generally larger than ordinary epidermal cells. At the junction with the sunken guard cells, the thickened walls of the subsidiary cells appear sharply thinned.

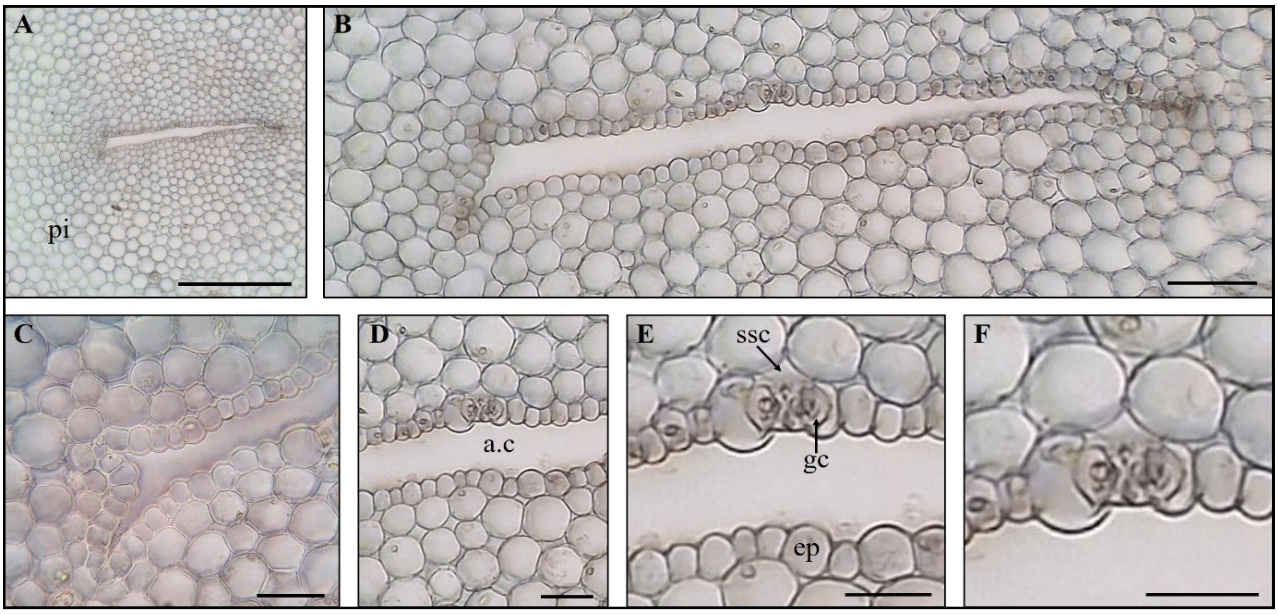


**Fig. 22.** Internal aerenchymal cavity in the stem, covered by epidermis and stomatal apparatus: *pi* – pith; *gc* – guard cells; *ssc* – sub-stomatal cavity; *ep* – epidermis; *a.c* – aerenchymal cavity; scale bar: *A* – 500 µm; *B* – 100 µm; *C*, *D* – 50 µm; *E*, *F* – 40 µm

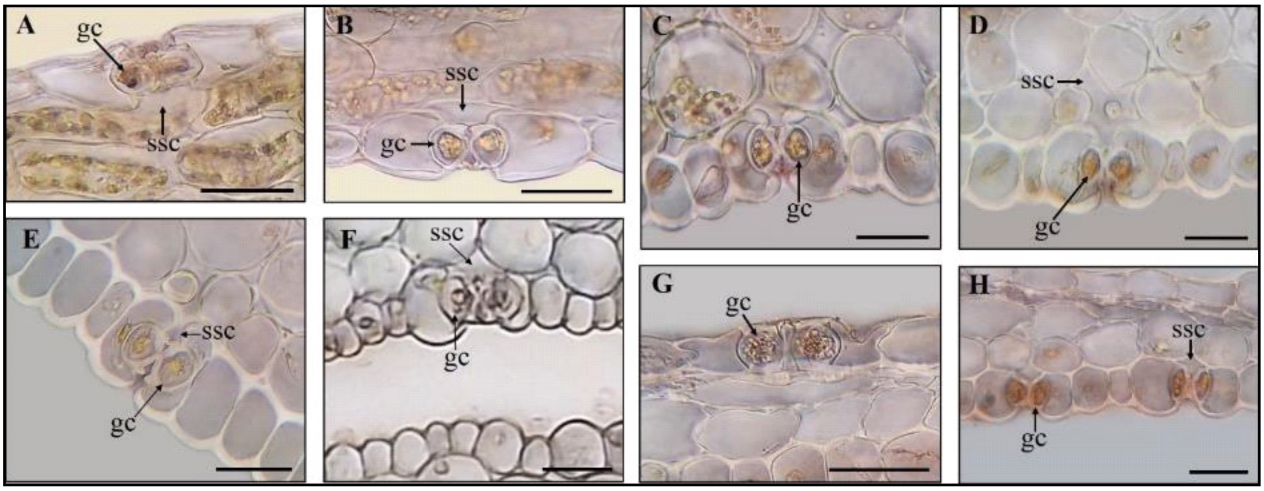


**Fig. 23.** Anomocytic stomata in the epidermis of different organs of the *Convallaria majalis*: *A* – in the adaxial epidermis of the leaf; *B* – in the abaxial epidermis of the leaf; *C* – in the lower epidermis of the petiole; *D* – in the outer epidermis of the sheath surrounding the stem in the adult phase; *E* – in the outer epidermis of the stem; *F* – in the inner epidermis of the stem; *G* – in the epidermis lining the inner side of the inner sheath surrounding the pip; *H* – in the epidermis lining the outer side of the outer sheath surrounding the pip; *gc* – guard cells; *ssc* – sub-stomatal cavity; scale bar – 30 μm

On the outer surface and within the internal aerenchyma of the stem, guard cells share a similar structure, but the subsidiary cells differ considerably. The outer epidermis of the stem consists of rhythmically arranged columnar cell series. The subsidiary cells of stomata positioned among these cells are narrow and elongated in the anticlinal direction, and the guard cells appear to be completely embedded within them. Conversely, the internal epidermis of the stem is composed of irregular, quadrangular, mosaic-like cells without wall thickening. Here, the stomatal complexes show asymmetrical subsidiary cells, with one being significantly larger. The guard cells are embedded between the two and are nearly equal in size and volume to the surrounding epidermal cells, although morphologically distinct. These chloroplast-rich guard cells have thickened walls on their opposing faces, from which papilla-like protrusions extend toward the internal and external epidermal surfaces. The internal stomatal apparatus formed on the stem's anisocytic or isodiametric epidermis represents a structurally atypical and morphogenetically significant localization.

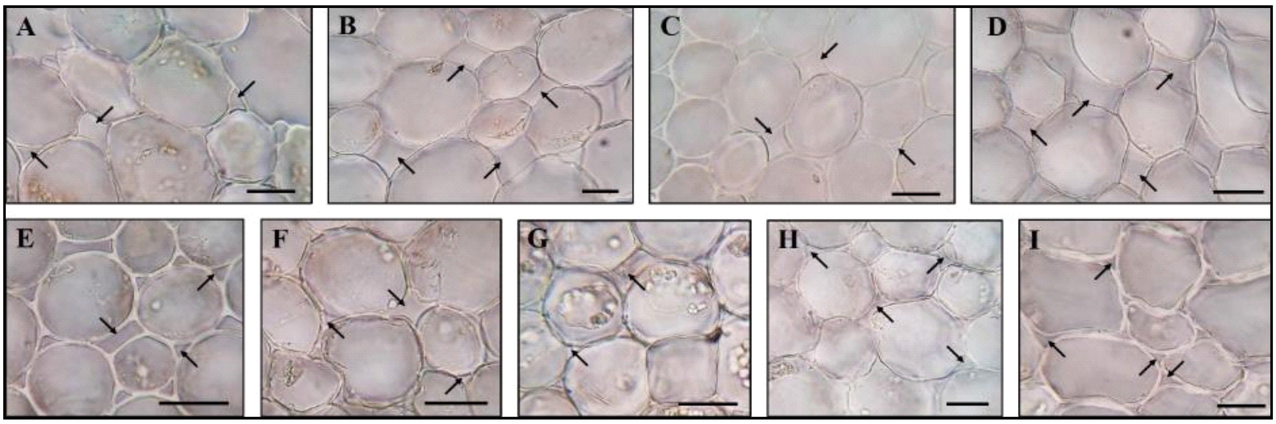


**Fig. 24.** Intercellular spaces in the parenchyma tissue in different organs of *Convallaria majalis* (marked with the arrows): in the petiole (*A*); in the sheath (*B*) surrounding the stem in the adult phase; in the cortical parenchyma (*C*) and pith parenchyma (*D*) of the stem; in the cortical parenchyma (*E*) and pith parenchyma (*F*) of the rhizome in the adult phase; in the cortical parenchyma (*G*) and pith parenchyma (*H*) of the rhizome in the juvenile phase; in the mesoderm (*I*) of the root; scale bar – 30 μm

The stomatal complexes observed on the epidermis of the inner sheath surrounding the developing shoot also display unique morphological features. Here, the guard cells are relatively large and round, while the subsidiary cells are morphologically indistinct from other epidermal cells. Because the subepidermal parenchyma is compact in this region, air chambers like those observed in other organs are absent. On the outer surface of the external sheath, the subsidiary cells are slightly larger than the surrounding epidermal cells, while the guard cells are comparatively smaller and more slender in oval shape. The morphology and localization of stomata in the stem of *C. majalis* vary across different regions, forming a heteromorphic and atypically localized stomatal system. The presence of an endoepidermal–stomatal structure within the stem constitutes a novel scientific finding, suggesting that this morphogenetically modified architecture is an adaptive response to specific physiological needs such as microventilation and internal gas regulation. Research also revealed that the vegetative organs of *C. majalis*, particularly the stem parenchyma, exhibit characteristic intercellular spaces (Fig. 24). These large, extensive cavities represent adaptive structures that enhance aeration and regulate the transpiration regime. However, anatomical analysis of the mesophyll structure indicated that intercellular spaces are less pronounced, likely due to the spatial organization of heteromorphic parenchyma cells. While gas exchange in most plant species predominantly occurs via the leaf, it appears that in *C. majalis* – where the leaf exhibits weak isolateral differentiation – ventilation is supported by the formation of large aerenchyma cavities in the stem, sheath, petiole, and central leaf region. This integrated function among organs represents a conservative adaptive strategy for life in shaded environments.

An asymmetric thickening of the endodermis was observed in the rhizome of *C. majalis* (Fig. 25A), a structural feature associated with the regulation of selective filtration. This unilateral endodermal thickening represents an adaptive response linked to hydrotropic and gravitropic stimuli. The species-specific endodermal architecture in the rhizome of *C. majalis* facilitates compensatory functionality by enhancing symplastic transport of water and ions while enabling lateral movement. Similar endodermal adaptations have been reported in *Asphodelus aestivus* (Sawidis et al., 2005), *Oryza sativa* (Aybek, 2016), and other species; however, this structural trait is described here for the first time in the medicinally important species *C. majalis*.

A comparative analysis of high-resolution photomicrographs of the *C. majalis* rhizome, captured using confocal laser scanning microscopy and available through online resources, further confirmed the presence of a cuticle layer. In particular, a micrograph published on the Shutterstock platform by neuroscientist Alexandros A. Lavdas (Shutterstock, 2019), working at the Eurac Research Center, displays fluorescently stained cross-sections of the rhizome, revealing distinctly luminescent tissue layers, including a prominently developed cuticular layer overlying the epidermis. These observations corroborate the findings of our anatomical investigation.

The rhizome of *C. majalis* exhibits both root- and stem-like features, although it is anatomically closer to the stem, as suggested by its parenchyma-dominated central region (Yeşil & Özhatay, 2021). Despite being stem-derived, the rhizome has evolved certain root-like features in response to its subterranean habit. Our study revealed a well-developed cuticle layer on the rhizome surface (Fig. 25B), consistent with its taxonomic classification as a monocot. In monocotyledonous species, secondary growth is typically limited or absent; therefore, the epidermis and associated cuticle serve as the primary protective layers against external stress. The thick cuticle plays a critical role in shielding the rhizome from abrasion caused by soil microorganisms and mechanical impact.

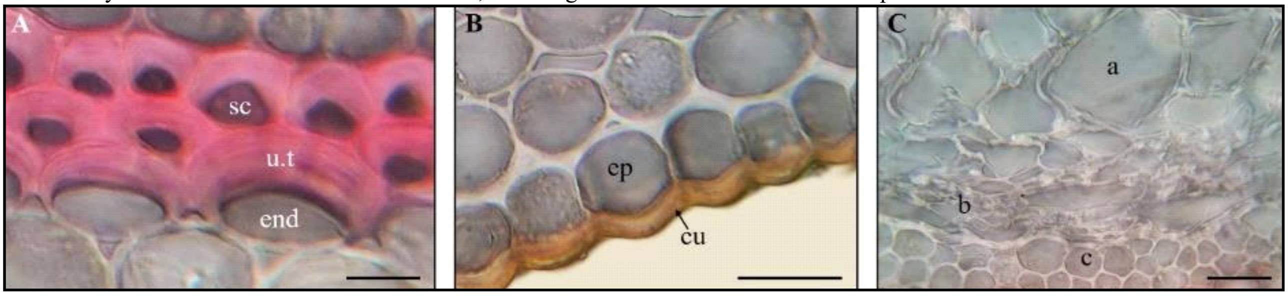


**Fig. 25.** Specific structures of *Convallaria majalis*: *A* – endodermal cell with unilateral thickened wall, supported by mechanical cells from the cortex side in the rhizome in the adult phase; *B* – thick cuticle on the surface of the epidermis of the rhizome in the adult phase; *C* – anisocytic morphological variation (*a*, *b*, *c*) of mesodermal cells in the root; *sc* – sclerenchyma; *end* – endodermis; *u.t* – unilateral thickened wall; *ep* – epidermis; *cu* – cuticle; scale bar: *A*, *B* – 30 μm; *C* – 50 μm

Functionally and anatomically, this feature is interpreted as an adaptive response to the short-lived nature of the rhizome. In *C. majalis*, the rhizome serves as a storage organ for nutrient reserves and supports seasonal growth strategies. The species is naturally adapted to shaded ecosystems characterized by relatively stable microclimates, and its rhizomes tend to be shallowly positioned in the soil. This facilitates its role as an energy reservoir during the growing season, enhances vegetative propagation, and enables rapid spread across the soil surface. However, its near-surface location also exposes the rhizome to fluctuating humidity, elevated temperatures, and ultraviolet radiation. Therefore, the species-specific development of a robust cuticle layer on epidermal cells likely functions to reduce water loss and enhance mechanical protection. Environmental stressors such as changes in soil moisture and microclimate conditions may further induce cuticle thickening as a protective adaptation (Yeats & Rose, 2013; Arya et al., 2021). The correlation between rhizome epigeicity and cuticular development can thus be interpreted as a clear case of adaptive anatomical modification.

Microscopic examination also revealed thickening of the inner epidermal wall in the rhizome, leading to the formation of collenchyma, which may be associated with the rhizome's proximity to the soil surface and exposure to environmental stress. Additionally, 2–3 subepidermal layers of collenchyma cells were observed. These collenchymatous layers appear to rest upon a developing exodermis, suggesting a defensive role in structural reinforcement. In this context, the inner epidermal collenchyma may regulate water balance as part of an adaptive mechanism. Given its shallow position, the rhizome is more vulnerable to mechanical stress and fluctuating moisture levels, and the observed inner wall thickening may serve as a defense response. Exodermal layers, characterized by suberized or lignified cell walls in many underground organs, were also identified in our anatomical analysis of the *C. majalis* rhizome. In the root, the disintegration of the epiblema and the temporary function of the exodermis as a protective tissue were observed. This structural transition is not associated with the onset of secondary development but is instead attributed to ontogenetic aging and functional adaptation. Considering the perennial nature of the species, the gradual loss of absorptive function in the root and the shift toward anchorage and storage functions render the epiblema physiologically unnecessary. Hence, the exodermis temporarily assumes its protective role.

The root of *C. majalis* exhibits a primary anatomical organization. Below the exodermis, a heterogeneous population of mesodermal cells was identified through microscopic analysis. Variation in cell size and shape delineates a hypodermal parenchymatous zone, comprising very large and very small isodiametric cells, as well as large, elongated cells with tapering ends (Fig. 25C). In shade-adapted plants such as *C. majalis*, this differentiation of parenchymal tissue represents a characteristic structural adaptation. The mesodermal cells displayed anisocytic morphological variation, marked by hypertrophied forms and ecological plasticity in cell size – features considered specific to the species. Additionally, small, elongated prosenchymatous cells were present in the mesodermal region, containing nongranular, light-colored, fluid-filled materials. Based on their cytological and morphological features, these cells were identified as secretory idioblasts or secondary metabolite storage cells (Crozier et al., 2006; Liu et al., 2023). These idioblasts are hypothesized to store biologically active compounds such as alkaloids, glycosides, and other phenolic metabolites, highlighting the pharmacological relevance of this tissue and its potential for further investigation. Similar idioblasts were also found near the sclerenchyma bundles of the stem sheath and at the interface with collenchyma (Fig. 26). The identification of such parenchymatous localizations for the first time in *C. majalis* represents a species-specific anatomical marker and provides novel insight into its systematic and functional characteristics as a pharmaco-anatomical trait.

Microscopic examinations of cross-sections of plant organs revealed the accumulation of ergastic and constitutional substances within various tissues. Investigations concerning their biochemical foundations have been documented across several scientific archives. For instance, Demir et al. (2022) studied a number of biochemical processes occurring in *Convallaria majalis,* isolating biologically active compounds of medicinal importance and evaluating their potential applications in both industry and biochemical systems. The plant specimens were collected during the flowering phase (April–May) from the Agyakha district in the Muğla region of Turkey. The authors identified the presence of volatile organic compounds such as citronellol, geraniol, and benzyl alcohol in the flowers. Additionally, the protease enzyme was purified and isolated, and it was suggested that these aromatic compounds could serve as active ingredients in various applications.

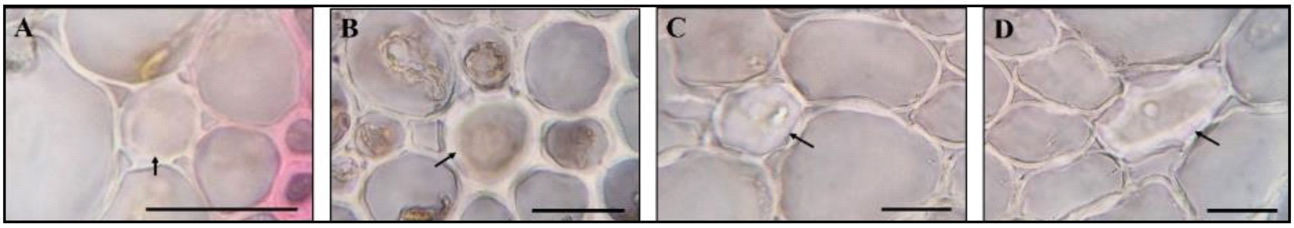

**Fig. 26.** Idioblast-type parenchymatous secretory cell (marked with the arrows): at the boundary with sclerenchyma (*A*) and collenchyma (*B*) of the sheath surrounding the stem in the adult phase; in the mesoderm (*C*, *D*) of the root; scale bar – 30 µm

Matsuo et al. (2017) also examined the biochemical composition of *C. majalis*, focusing on the anticancer properties of purified organic substances. Plant samples were supplied by Richters Co., Ltd. Their study identified the presence of steroidal glycosides, which have been confirmed in previous research to possess potent anticancer effects. While prior studies have elucidated the biochemical composition of bioactive constituents in *C. majalis*, they have not addressed their tissue-specific localization or detailed distribution at a microscopic level. This gap limits our understanding of which plant organs are most efficient as raw material sources for therapeutic use and the functional role of these metabolites. In our study, we visualized the accumulation of bioactive compounds within tissues (e.g., parenchyma, vascular elements), enabling us to trace their biosynthetic and accumulation dynamics. For example, in *C. majalis* leaves, photosynthetic substances were observed within idioblast cells of the parenchymal tissue. This correlates with chloroplast localization and intracellular metabolic adaptation. Such structural features reflect the plant's adaptation to shade tolerance and may serve critical functions such as temporary storage of photosynthetic products and regulation of carbon metabolism. At the cytological level, these processes influence pigment balance depending on light conditions, representing a complex interaction between the plant’s morphophysiological traits and its ecologically variable environment (Bertoft, 2017; Apriyanto et al., 2022). This adaptation mechanism is especially critical under ecological stress, such as low light intensity in shaded habitats.

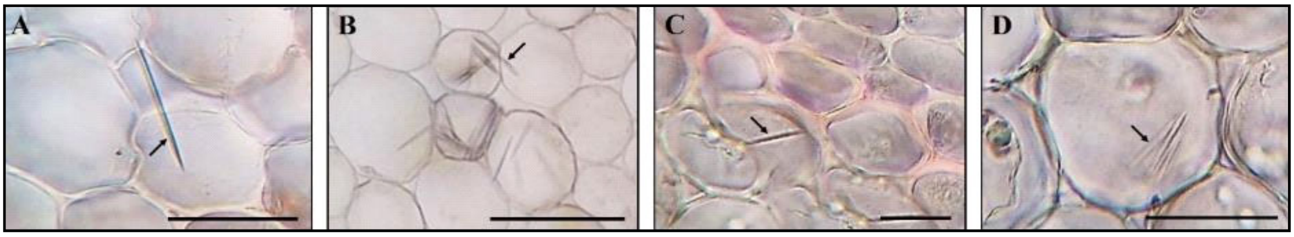

**Fig. 27.** Raphide crystals in different organs of *Convallaria majalis* (marked with the arrows): in the parenchyma (*A*) of the outer sheath surrounding the pip; in the cortical parenchyma (*B*) of the stem; in the endodermis cell (*C*) and cortical parenchyma (*D*) of the rhizome in the juvenile phase; scale bar – 30 µm

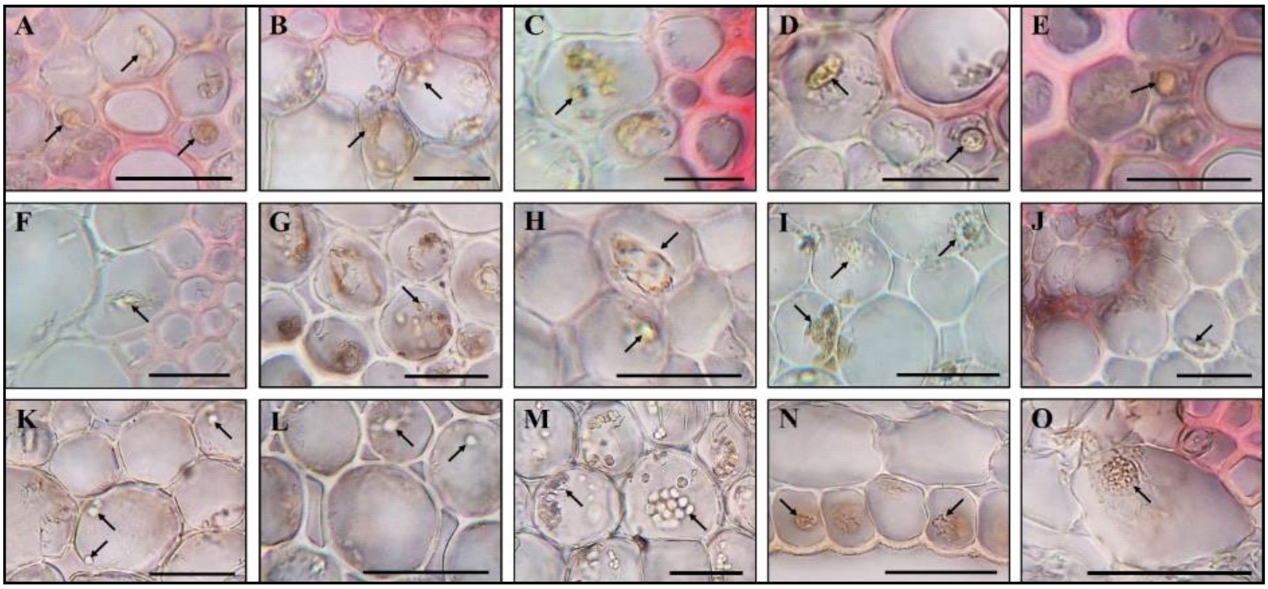

**Fig. 28.** Ergastic and constitutional substances in different organs of *Convallaria majalis* (marked with the arrows): in the parenchyma cells at the boundary with xylem (*A*) and sclerenchyma (*B*, *C*) of the leaf; in the parenchyma cells at the boundary with xylem (*D*, *E*) of the petiole; in the parenchyma cells at the boundary with sclerenchyma (*F*) and collenchyma (*G*) of the sheath surrounding the stem in the adult phase; in the pith (*H*) and cortical parenchyma (*I*) of the stem; in the pith parenchyma cells adjacent to the xylem (*J*, *K*) and in the cortical parenchyma (*L*) of the rhizome in the adult phase; in the cortical parenchyma (*M*) of the rhizome in the juvenile phase; in the epidermis cells (*N*) lining the outer side of the inner sheath surrounding the pip; in the parenchyma cell (*O*) adjacent to the sclerenchyma of the inner sheath surrounding the pip; scale bar – 30 µm

Microscopic observations of *C. majalis* further revealed the accumulation of granular bodies – likely proteinaceous or starch-based – within the phloem, adjacent parenchymatic cells, and occasionally libriform cells. These reserve substances were predominantly concentrated within the phloem tissues. Oxalate crystals were observed in the primary parenchymal cells of the stem, suggesting the plant's capacity to adapt to low-light environments through physiological stress responses. Raphide crystals – composed mainly of calcium oxalate – were identified in the cortical parenchyma of the stem, in the rhizome during its juvenile phase (in parenchymal and endodermal cells), and in the sheaths covering the primary seedling (Fig. 27). The formation of these crystals is associated with calcium ion regulation and, in shade-tolerant mesophytes such as *C. majalis*, may support ionic balance. Raphides may also contribute to water regulation and intracellular osmotic balance (Salam et al., 2023; Dixon & Dickinson, 2024). Given that the cortex predominantly consists of parenchymal cells, raphide formation is likely to influence the metabolic activity of these cells. Localized accumulations of ergastic substances (i.e., reserve compounds) in the vegetative organs of *C. majalis* were documented (Fig. 28), indicating a metabolic adaptation mechanism. These accumulations may represent an adaptive structural feature that supports metabolism and energy storage under shaded conditions (Korniyevskyi & Korniyevska, 2017). To further characterize the chemical nature of these compounds, chromatographic analyses by pharmaceutical experts are recommended.

The findings of this study contribute to a broader understanding of structural-physiological functionality that may occur under limited light regimes in similar environmental contexts, not only at the species level but also among populations of other taxa (Shafiq et al., 2020).

## Conclusions

As a result of the present study, a comprehensive eco-anatomical identification was conducted for the first time on the vegetative organs of the sciophyte species *C. majalis*. The leaf mesophyll did not differentiate into a fully isolateral structure but displayed dorsoventral characteristics along with zonal parenchymatic modifications, which are interpreted as indicative of adaptation to shaded environments. In the stem parenchyma, the presence of an endo-aerenchymal stomatal structural complex was identified, representing a novel contribution to the field of botany at the international level. Lignified cell walls were observed in the phloem region, and hypertrophied heteromorphic cells were recorded in the mesoderm. As a result, anisocytic morphological variations were documented within the sub-exodermal histological complex, as confirmed by photomicrography. Parenchyma tissues were also identified in the stem. In the root, ontogenetic degeneration of the epiblema tissue led to the compensatory protective function of the exodermis, while unilateral wall thickening in endodermal cells was considered a diagnostic feature. The accumulation of photosynthetic products in the perivacuolar zones, the localization of ergastic substances in the phloem and parenchyma tissues, the arrangement of sclerenchyma around the vascular system, and the sequential alignment of conductive bundles in lateral regions were all associated with functional zonation. Furthermore, trihedral–hexahedral and polygonal variations of the vascular system were evaluated as indicators of tissue differentiation and structural modification. Intercellular spaces were recorded in vegetative organs, particularly in the stem. The findings of this study bear fundamental and applied significance in various fields including biodiversity, pharmacopoeia, autoecology, plant physiology, and molecular botany (metabolomics, marker identification), among others.

## References


Anurag, K., Jangid, P. P., Marimuthu, S., Gurav, A. M., Srikanth, N., Mangal, A. K., Venkateshwarlu, B., & Shiddamallayya, N. (2023). Identification and authentication of *Agnimantha* plant species used in Ayurveda on the basis of anatomical and molecular phylogenetic analysis. Plant Science Today, 10(4), 26–38.

Apriyanto, A., Compart, J., & Fettke, J. (2022). A review of starch, a unique biopolymer – structure, metabolism and in planta modifications. Plant Science, 318, 111223.

Arya G. C., Sarkar S., Manasherova E., Aharoni A., Cohen H. (2021). The plant cuticle: An ancient guardian barrier set against long-standing rivals. Frontiers in Plant Science, 12, 663165.

Aybek, M. (2016). Root anatomical plasticity in response to salt stress under real and full-season field conditions and determination of new anatomic selection characters for breeding salt-resistant rice (*Oryza sativa* L.). Trakya University Journal of Natural Sciences, 17(2), 87–104.

Belaeva, T. N., & Butenkova, A. N. (2018). Comparative analysis of the leaf anatomy of *Echinacea purpurea* and *E. pallida*. Biosystems Diversity, 26(2), 77–84.

Bertoft, E. (2017). Understanding starch structure: Recent progress. Agronomy, 7(3), 56.

Bessonova, V. P., & Yakovleva-Nosar, S. O. (2014). Fiziolohiya roslyn [Plant physiology]. Svidler A. L., Dnipro (in Ukrainian).

Boubetra, K., Amirouche, N., & Amirouche, R. (2022). Morpho-anatomical diversity of five species of genus *Asparagus* (Asparagaceae) from Algeria. Acta Botanica Croatica, 81(2), 168–176.

Bozdağ, B., Kocabaş, O., & Özdemir, C. (2016). Bitki anatomisi çalışmalarında el kesitleri için yeni boyama yöntemi [A new staining method for hand sections in plant anatomy studies]. Marmara Pharmaceutical Journal, 20(2), 184–190 (in Turkish).

Bulavin, I. V. (2013). Anatomična kharakterystyka stebel odnorichnykh paghoniv sukulentnykh roslyn rodu *Euphorbia* L. (Euphorbiaceae) [Anatomical characteristics of stems of annual shoots of succulent plants of the genus *Euphorbia* L. (Euphorbiaceae)]. Ukrainskyi Botanichnyi Zhurnal, 70(1), 45–53 (in Ukrainian).

Bulavin, I. V. (2015). Anatomiia ta ultrastruktura koreniv *Arabidopsis thaliana* v kulturi *in vitro* pid vplyvom klinostatuvannia [Anatomy and ultrastructure of *Arabidopsis thaliana* roots in *in vitro* culture under clinorotation]. Ukrainskyi Botanichnyi Zhurnal, 72(2), 180–185 (in Ukrainian).

Chen, J., Wu, S., Dong, F., Li, J., Zeng, L., Tang, J., & Gu, D. (2021). Mechanism underlying the shading-induced chlorophyll accumulation in tea leaves. Frontiers in Plant Science, 12, 779819.

Cormack, R. G. H. (1962). Alteration of leaf size and structure in *Convallaria majalis* caused by extreme shade. Canadian Journal of Botany, 40(3), 383–387.

Criswell, S., Gaylord, B., & Pitzer, C. R. (2025). Histological methods for plant tissues. Journal of Histotechnology, 48(1), 58–67.

Crozier, A., Clifford, M. N., & Ashihara, H. (Eds.). (2006). Plant secondary metabolites: Occurrence, structure and role in the human diet. Blackwell Publishing, Oxford.

Da Silva, C. J., De Lima, L. H. F., De Paiva, P. M., Maia, L. M., Rocha, R. E. de O., De Souza, P. T. D., & Carvalho, D. A. de C. A. (2020). An inexpensive and environmentally friendly staining method for semi-permanent slides from plant material probed using anatomical and computational chemistry analyses. Rodriguésia, 71, e01662018.

Demir, N., Daşdemir, S. N., Kaplan, A., & Demir, Y. (2022). Determination of bioactivities of *Convallaria majalis* L. (lily of the valley), isolating pharmaceutical active ingredients and investigation its industrial usage. Middle East Journal of Science, 8(2), 122–137.

Dixon, R. A., & Dickinson, A. J. (2024). A century of studying plant secondary metabolism – from “what?” to “where, how, and why?” Plant Physiology, 195, 48–66.

Dörken, V. M., & Lepetit, B. (2018). Morpho-anatomical and physiological differences between sun and shade leaves in *Abies alba* Mill. (Pinaceae, Coniferales): A combined approach. Plant, Cell and Environment, 41(7), 1683–1697.

Engin, H., Kuzucu, F. C., & Gökbayrak, Z. (2024). Odun çeliklerinin mikroskobik inceleme ve görüntülenmesinde farklı boyama tekniklerinin kullanımı üzerine araştırmalar [Research on the use of different staining techniques in microscopic examination and imaging of woody cuttings]. ÇOMÜ Ziraat Fakültesi Dergisi, 12(1), 108–120 (in Turkish).

Harb, R. K., El-Kobisy, O. S., & Desoukey, S. F. (2016). Anatomical and chemical investigations on *Asparagus officinalis* L. (Asparagaceae). Arab University Journal of Agricultural Sciences, Ain Shams University, Cairo, 24(2), 655–664.

Hardtke, C. S. (2023). Phloem development. New Phytologist, 239, 852–867.

Huang, B., & Yeung, E. (2015). Chemical and physical fixation of cells and tissues: An overview. In: Yeung, E., Stasolla, C., Sumner, M., & Huang, B. (Eds.). Plant microtechniques and protocols. Springer, Cham. Pp. 23–43.

Ibadullayeva, S. J. (2024). Traditional folk medicine of Azerbaijanis [Traditional folk medicine of Azerbaijanis]. Savad, Baku (in Azerbaijani).

Jambor, H., Antonietti, A., Alicea, B., Audisio, T. L., Auer, S., Bhardwaj, V., Burgess, S. J., Ferling, I., Gazda, M. A., Hoeppner, L. H., Ilangovan, V., Lo, H., Olson, M., Mohamed, S. Y., Sarabipour, S., Varma, A., Walavalkar, K., Wissink, E. M., & Weissgerber, T. L. (2021). Creating clear and informative image-based figures for scientific publications. PLoS Biology, 19(3), e3001161.

Kabus, I. (2015). *Convallaria majalis* – Maiglöckchen (Convallariaceae), Giftpflanze des Jahres 2014 [*Convallaria majalis* – lily of the valley (Convallariaceae), poisonous plant of the year 2014]. Jahrbuch des Bochumer Botanischen Vereins, 6, 188–191 (in German).

Korniyevskyi, Y. I., & Korniyevska, V. H. (2017). Anatomiya roslyn [Plant anatomy]. Zaporizhzhia State Medical University, Zaporizhzhia (in Ukrainian).

Kucharczyk, I., Kucharczyk, M., & Tchórzewska, D. (2022). The life cycle of *Ctenothrips distinctus* (Uzel, 1895) (Insecta: Thysanoptera) and its influence on the host plant *Convallaria majalis* L. Folia Biologica (Kraków), 70(4), 185–200.
Liu, S., Zhang, Q., Kollie, L., Dong, J., & Liang, Z. (2023). Molecular networks of secondary metabolism accumulation in plants: Current understanding and future challenges. Industrial Crops and Products, 201, 116901.
Makruf, M. I., Maryani, & Susandarini, R. (2024). Comparative study of the leaf anatomy of *Dendrobium* species (Orchidaceae) from South Kalimantan, Indonesia and its taxonomic significance. Plant Science Today, 11(2), 742–749.
Matsuo, Y., Shinoda, D., Nakamaru, A., Kamohara, K., Sakagami, H., & Mimaki, Y. (2017). Steroidal glycosides from *Convallaria majalis* whole plants and their cytotoxic activity. International Journal of Molecular Sciences, 18(11), 2358.
Middleton, L. (2001). Shade-tolerant flowering plants: Adaptations and horticultural implications. Acta Horticulturae, 552, 95–102.
Nyzhnyk, T. P., Kots, S. Y., Pukhtaievych, P. P., Kots, T. A., & Vegera, L. V. (2024). Chelated forms of trace elements improve antioxidant properties and nodulation potential of soybean-*Bradyrhizobium* symbiosis under insufficient water conditions. Biosystems Diversity, 32(2), 252–259.
Popova, O. M. (2017). Anatomiya roslyn [Plant anatomy]. Odesa I. I. Mechnikov National University, Odesa (in Ukrainian).
Pradhan Mitra, P., & Loqué, D. (2014). Histochemical staining of *Arabidopsis thaliana* secondary cell wall elements. Journal of Visualized Experiments, 87, e51281.
Qurbanov, E. M. (2024). Azərbaycanın bitki örtüyü [Vegetation of Azerbaijan]. Bakı, Elm (in Azerbaijani).
Rajput, K. S., Kapadane, K. K., Ramoliya, D. G., Thacker, K. D., & Gondaliya, A. D. (2022). Inter- and intraxylary phloem in vascular plants: A review of subtypes, occurrences, and development. Forests, 13(12), 2174.
Rezanejad, F., Ganjalikhani Hakemi, F., & Bakhtyari, F. (2023). Adaptive morpho-anatomical characteristics of leaves and cones in *Juniperus seravschanica* Kom.: Studies of polyphenolic parenchyma cells, secretory tissues, sclereids and tracheids. Acta Biologica Cracoviensia Series Botanica, 65(2), 49–61.
Ružička, K., Ursache, R., Hejátko, J., & Helariutta, Y. (2015). Xylem development – from the cradle to the grave. New Phytologist, 207(3), 519–535.
Ryabchuk, V. P., & Perekhodko, O. M. (2004). Konvaliya zvychaina (*Convallaria majalis* L.) v umovakh zakhodu Ukrayiny [Lily of the valley (*Convallaria majalis* L.) in the Western Ukraine]. Naukovyi Visnyk Ukrayins'kogo Derzhavnogo Lisotekhnichnogo Universytetu, 14(1), 8–12 (in Ukrainian).
Saeidi Mehrvarz, S., & Moharami, E. (2016). Anatomical study on some species of genus *Cyperus* in Northern Iran. Ukrainian Botanical Journal, 73(3), 234–238.
Salam, U., Ullah, S., Tang, Z.-H., Elateeq, A. A., Khan, Y., Khan, J., Khan, A., & Ali, S. (2023). Plant metabolomics: An overview of the role of primary and secondary metabolites against different environmental stress factors. Life, 13(3), 706.
Sarapan, A., Hodkinson, T. R., & Suwanphakdee, C. (2023). Assessment of morphological, anatomical and palynological variation in the medicinal plant *Disporopsis longifolia* Craib (Asparagaceae) for botanical quality control. Plants, 12(2), 259.
Sardarova, A. S. (2024). The anatomical characteristics of the vegetative and generative organs of the medicinal *Silybum marianum* L. spread in the mountainous region of the Lesser Caucasus. Advances in Biology and Earth Sciences, 9(3), 381–388.
Sardarova, A. S. (2025a). Comparative ecological anatomical characteristics of generative and vegetative organs of the medicinally important plant *Fragaria vesca* L. (Rosaceae Juss.) under *in situ* and *ex situ* conditions. Transactions of the Institute of Molecular Biology and Biotechnologies, 9(1), 17–37.
Sardarova, A. S. (2025b). Comparative ecological anatomical study of the structural adaptation of the medicinally important plant *Salvia nemorosa* L. under *in situ* and *ex situ* conditions. Acta Botanica Caucasica, 4(2), 81–100.
Sardarova, A. S. (2025c). Ecological and anatomical characteristics and tolerance of *Salsola nodulosa* Iljin and *Zygophyllum fabago* L. species under environmental pressures in arid and saline ecosystems. Acta Botanica Caucasica, 4(1), 106–123.
Sardarova, A., & Ibadullayeva, S. (2025). Ecological anatomical study of structural-plastic response reactions of the medicinally important species *Laurus nobilis* (Lauraceae) in various ecological conditions. Plant and Fungal Research, 8(1), 23–35.
Sawidis, T., Kalyva, S., & Delivopoulos, S. (2005). The root-tuber anatomy of *Asphodelus aestivus*. Flora, 200, 332–338.
Schwartau, V. V., Mykhalska, L. M., Makoveychuk, T. I., & Tretiakov, V. O. (2024). Chlorine in plant life. Biosystems Diversity, 32(4), 445–469.
Shafiq, I., Hussain, S., Raza, M., Iqbal, N., Asghar, M., Yuan-Fang, F., Mumtaz, M., Shoaib, M., Ansar, M., Manaf, A., Yang, W.-Y., & Feng, Y. (2020). Crop photosynthetic response to light quality and light intensity. Journal of Integrative Agriculture, 19, 2–21.
Théroux-Rancourt, G., Herrera, J. C., Voggeneder, K., De Berardinis, F., Luijken, N., Nocker, L., Savi, T., Scheffknecht, S., Schneck, M., & Tholen, D. (2023). Analyzing anatomy over three dimensions unpacks the differences in mesophyll diffusive area between sun and shade *Vitis vinifera* leaves. AoB Plants, 15(2), plad001.
Ulcay, S. (2022). Anatomy, palynology, seed and leaf micromorphology of Turkish endemic *Allium brevicaule* Boiss. & Balansa and *Allium scorodoprasum* ssp. *rotundum* (L.) Stearn. Acta Biologica Cracoviensia Series Botanica, 64(1), 27–38.
Uma, M. M., & Düzenli, A. (2012). Bitki toplama, teşhis ve herbaryum teknikleri [Plant collection, identification, and herbarium techniques]. Fen ve Mühendislik Bilimleri Dergisi, 28(3), 153–162 (in Turkish).
Voxeur, A., Wang, Y., & Sibout, R. (2015). Lignification: Different mechanisms for a versatile polymer. Current Opinion in Plant Biology, 23, 83–90.
Weng, J.-K., Li, X., Stout, J., & Chapple, C. (2008). Independent origins of syringyl lignin in vascular plants. Proceedings of the National Academy of Sciences, 105(22), 7887–7892.
Xu, T., Li, Z., Bao, S., Su, Y., Su, Z., Zhi, S., & Zheng, E. (2023). Xylem vessel type and structure influence the water transport characteristics of *Panax notoginseng*. PLoS One, 18(3), e0281080.
Yeats, T. H., & Rose, J. K. C. (2013). The formation and function of plant cuticles. Plant Physiology, 163, 5–20.
Yeşil, Y., & Özhatay, F. N. (2021). Scape, rhizome and root anatomy of *Polygonatum* species from Turkey. European Journal of Biology, 80(2), 164–172.